A model analysis of the effects of nonspecific monoterpenoid storage in leaf tissues on emission kinetics and composition in Mediterranean sclerophyllous *Quercus* species

Ülo Niinemets
Department of Plant Physiology, Institute of Molecular and Cell Biology, Tartu, Estonia

Markus Reichstein
Department of Plant Ecology, University of Bayreuth, Bayreuth, Germany

Received 3 May 2002; revised 28 June 2002; accepted 16 July 2002; published 4 December 2002.

[1] Although monoterpenoid-emitting *Quercus* species lack specific terpene storage structures, they may store monoterpenoids in nonspecific leaf compartments. To determine whether such storage may influence emission responses to diurnal changes in environmental factors, a dynamic emission model including ''fast'' and ''slow'' storage pools in parallel was constructed. Existence of two storage pools was inferred from the circumstance that monoterpene efflux from darkened leaves was poorly described by single-exponential decay relationship, but was well parameterized by double exponentials. Simulations indicated that nonspecific terpenoid storage may significantly alter daily monoterpenoid emission both at leaf and canopy scales. The model also described shifts in fractional monoterpenoid composition after changes in environmental factors that cannot be explained by current algorithms. Time constants for the ''fast'' pool were negatively associated with monoterpenoid equilibrium gas/water partition coefficient (*H*), suggesting that the ''fast'' pool is in leaf liquid phase. The time constants for the ''slow'' pool were independent of *H*, but scaled positively with monoterpenoid octanol/water partition coefficient, indicating that this pool is in lipid phase. Based on tentative pool locations and monoterpenoid physico-chemical characteristics, time constants of various pools were computed using a flow/conductance model. Although the time constants were correlated, the theoretical estimates were larger than those derived empirically. Nonhomogeneous monoterpenoid distribution, aggregation within leaf liquid phase, and adsorption to apoplast surfaces that all decrease the area for diffusion and decrease the effective diffusion coefficients likely explain this discrepancy. We conclude that physico-chemical models are needed to parameterize nonspecific storage effects on monoterpene emission dynamics and emission composition. *INDEX TERMS:* 0315 Atmospheric Composition and Structure: Biosphere/atmosphere interactions; 0365 Atmospheric Composition and Structure: Troposphere—composition and chemistry; 1615 Global Change: Biogeochemical processes (4805); 1610 Global Change: Atmosphere (0315, 0325); *KEYWORDS:* biological controls, dynamic model, Henry's law constant, monoterpenoid emission, monoterpenoid storage, octanol/water partition coefficient, *Quercus ilex*

Citation: Niinemets, Ü., and M. Reichstein, A model analysis of the effects of nonspecific monoterpenoid storage in leaf tissues on emission kinetics and composition in Mediterranean sclerophyllous *Quercus* species, *Global Biogeochem. Cycles*, *16*(4), 1110, doi:10.1029/2002GB001927, 2002.

1. Introduction

[2] Volatile organic compounds play an important role in tropospheric ozone forming reactions [*Fehsenfeld et al.*, 1992; *Fuentes et al.*, 2000] and serve also as condensation nuclei in aerosol formation [*Pio et al.*, 2001]. At the global scale, model simulations suggest that biogenic emission of volatile organic compounds exceeds the anthropogenic emission [*Müller*, 1992; *Guenther et al.*, 1995]. However, there are still large uncertainties in estimations of volatile compound fluxes, because many aspects of biological controls on volatile emissions are still not entirely understood.

[3] Many plant species are strong emitters of monoterpenoids [*Fuentes et al.*, 2000; *Geron et al.*, 2000; *Guenther et al.*, 2000]. In conifers, which possess extensive storage pools of monoterpenoids in resin ducts, the diffusion flux from the pools is suggested to control the monoterpenoid emission rate

0886-6236/02/2002GB001927

[*Tingey et al.*, 1991; *Guenther et al.*, 1993]. Thus, in the current conifer' emission models, the monoterpene emission rates are driven only by changes in leaf temperature [*Guenther et al.*, 1993, 2000; *Lerdau et al.*, 1994; *Monson et al.*, 1995], assuming that the efflux from the pools is always in a steady state. However, there is a wide range of monoterpene emitting broad-leaved species [*Guenther et al.*, 1996; *Loreto et al.*, 1996a, 1996b; *Schuh et al.*, 1997; *Benjamin and Winer*, 1998; *Hakola et al.*, 1998] that lack specialized monoterpene-storage compartments within the leaves. In these species, monoterpenoid emission rates depend not only on temperature, but also on incident irradiance [*Loreto et al.*, 1996c; *Bertin et al.*, 1997; *Schuh et al.*, 1997; *Staudt and Bertin*, 1998] similarly to foliar isoprene emission rates [*Monson and Fall*, 1989; *Guenther et al.*, 1991].

[4] Previous simulation studies [*Bertin et al.*, 1997; *Ciccioli et al.*, 1997; *Kesselmeier et al.*, 1998; *Niinemets et al.*, 2002c] have used various isoprene emission algorithms [*Guenther et al.*, 1993; *Niinemets et al.*, 1999] to describe the diurnal variability in monoterpenoid emission rates in broad-leaved species. Although modeling monoterpene emission analogously to isoprene provides qualitatively good fits to the data in some instances, poorly understood variances on the order of 30–50% are a rule rather than an exception in such simulations [*Bertin et al.*, 1997; *Kesselmeier et al.*, 1997; *Peñuelas and Llusià*, 1999a, 1999b; *Sabillón and Cremades*, 2001]. The low modeling power of simple empirical algorithms driven only by incident irradiance and leaf temperature can partly be explained by water stress effects on volatile isoprenoid emission [*Sharkey and Loreto*, 1993; *Bertin and Staudt*, 1996; *Moncrieff et al.*, 1997; *Peñuelas and Llusià*, 1999a, 1999b] either due to decreases in isoprene and monoterpenoid synthase activities, or due to limited carbon and energy supply for isoprenoid synthesis [*Niinemets et al.*, 1999, 2002c].

[5] Apart from the stress effects, physico-chemical characteristics of monoterpenoids differ from those of isoprene. Thus, the emission kinetics of isoprene and monoterpenes may not necessarily be identical. In particular, the saturated partial pressure of monoterpenoids on the order of 0.02–0.6 kPa at 25°C is considerably lower than that of isoprene of 73.6 kPa at 25°C [*Mackay and Shiu*, 1981; *Howard and Meylan*, 1997; *Daubert et al.*, 1998; *Weitz and Loser*, 1998] (see also R. L. Brown and S. E. Stein, Boiling point data, in NIST Chemistry WebBook, NIST Standard Reference Database Number 69, edited by P. J. Linstrom and W. G. Mallard, National Institute of Standards and Technology, Gaithersburg, Md., available at http://webbook.nist.gov, July, 2001) and monoterpene molecules are also larger and diffuse more slowly than the isoprene molecules. This suggests that depending on the partitioning of diffusion limitations between lipid, liquid, and gas phases, the monoterpenoid emission rates may occasionally be limited by volatility and intraleaf diffusion also in species lacking specialized foliage monoterpene-storage compartments. Accordingly, the assumption of instantaneous light and temperature response that may be germane for more volatile isoprene may be inherently inappropriate for monoterpenoids, leading to significant errors in simulations of monoterpene emission.

[6] Several lines of evidence indicate that there may be a certain foliar monoterpene storage pool even in species lacking specific storage compartments within the leaves. (1) In experimental studies, terpenoid emission does not respond instantly, but with a time-lag after illumination of darkened leaves. Maximum values of emission are observed after several hours of constant illumination, and terpene emission does not come to an immediate halt after switching off the light [*Bertin and Staudt*, 1996; *Loreto et al.*, 1996a, 1996c, 2000; *Ciccioli et al.*, 1997; *Hansen and Seufert*, 1999]. Given that the biochemical regulation of isoprenoid synthesis is assumed to be very fast [*Logan et al.*, 2000; *Singsaas and Sharkey*, 2000], and the foliar pools of photosynthetic intermediates as well as ATP and NADPH contents are generally small [*Laisk et al.*, 1984; *von Caemmerer and Edmondson*, 1986; *Loreto and Sharkey*, 1993], such delayed responses hint at filling up and emptying of nonspecific terpene storage pools in the leaves. These delayed emission responses are further corroborated by slow monoterpene labeling and unlabeling kinetics in ^{13}C-feeding experiments [*Loreto et al.*, 1996a, 1996b, 2000]. (2) In the broad-leaved emitting species, there are significant night emissions from the leaves [*Ciccioli et al.*, 1997; *Schuh et al.*, 1997; *Loreto et al.*, 2000; *Niinemets et al.*, 2002a] that are not in accord with a complete lack of foliar monoterpene storage. (3) Anomalous responses of monoterpenoid emission rates to light and temperature—e.g., bursts of monoterpenoid emission after rapid changes in leaf temperature [*Ciccioli et al.*, 1997] as well as in hot days following cool days [*Niinemets et al.*, 2002a, 2002c]—are often observed in field studies [*Ciccioli et al.*, 1997; *Peñuelas and Llusià*, 1999b; *Niinemets et al.*, 2002a, 2002c], and cannot be explained by current emission algorithms. (4) Fumigation of leaves of terpene-emitting and nonemitting species with exogenous monoterpenes leads to significant monoterpenoid efflux from the leaves of both emitting and nonemitting species. Such emission fluxes are measurable for more than 12 h after the fumigation treatment [*Delfine et al.*, 2000], conclusively demonstrating that the leaves of species without specific storage compartments may still have a significant capacity for monoterpene storage. Finally, (5), direct measurements of intraleaf monoterpenoid contents indicate that monoterpene emission may continue with a maximal rate at the expense of the nonspecific storage for at least 10–15 min without any de novo synthesis [*Loreto et al.*, 1998]. These observations collectively imply that nonspecific storage effects may be significant, and consequently, may importantly alter monoterpenoid emission dynamics. Because environmental factors rapidly fluctuate during the day as well as between the days, consideration of such effects can be particularly relevant for simulation of diurnal time-courses of monoterpenoid emissions. Existence of a temporal storage in the leaves suggests that dynamic models may be required to improve the correspondence between experimental observations and model estimates.

[7] In a previous study [*Niinemets et al.*, 2002c], we demonstrated that a steady-state biochemical model coupling terpene production rate to the rate of photosynthetic electron transport may be successfully employed to simulate the emission in dependence on incident light and leaf temperature in Mediterranean sclerophyllous monoterpene-emitting

species *Quercus coccifera* L. and *Quercus ilex* L. [*Loreto et al.*, 1996a, 1996b, 1996c] that lack specialized terpene-storage compartments within the leaves. In the current study, we develop a phenomenological model (1) to explore the extent to which the emission from nonspecific storage may alter the emission kinetics in these species, and (2) to determine how long the emission from the pools can sustain foliar terpene efflux. We used the data of *Loreto et al.* [1996a] for model testing. Specifically, time-lags between the onset of emission and reaching a steady state, as well as the time-dependent decreases in terpene efflux from darkened leaves were employed for model parameterization. The kinetic data of terpene-release from terpene-fumigated leaves of *Q. suber* [*Delfine et al.*, 2000] were also analyzed. Although the leaves of *Q. suber* are morphologically homologous to other Mediterranean evergreen sclerophyllous *Quercus* species, *Q. suber* is a monoterpene nonemitter.

[8] In addition to reliable modeling of temporal changes in total terpene fluxes, it is also relevant to simulate time- and environment-dependent variabilities in composition of emitted monoterpenes, because the atmospheric life-times as well as reactivity in ozone-forming reactions vary more than two orders of magnitude between various monoterpenes [*Fehsenfeld et al.*, 1992]. In Mediterranean monoterpene emitting *Quercus* species, at least 22 different monoterpenoids have been observed in the emission patterns (see *Staudt et al.* [2001] and *Niinemets et al.* [2002c] for a review). Given that there is a broad variation in terpene solubilities, vapor pressures and diffusion coefficients [*Howard and Meylan*, 1997], the degree to which various monoterpenoids are stored should differ between the monoterpenoids. Thus, changes in environmental factors may alter the emission of various monoterpenes to a different extent, and there may be relevant diurnal alterations in fractional composition of emitted monoterpenoids. Therefore, a further task of our study (3) was to investigate the relationships between monoterpene physico-chemical characteristics and the storage pool time constants, and to determine whether differences in monoterpenoid physico-chemical variables may lead to altered composition of emissions. We (4) constructed an extensive data set of physico-chemical characteristics of monoterpenoids, and using the resistance/flow models determined the most critical variables that affect the monoterpenoid diffusion flux.

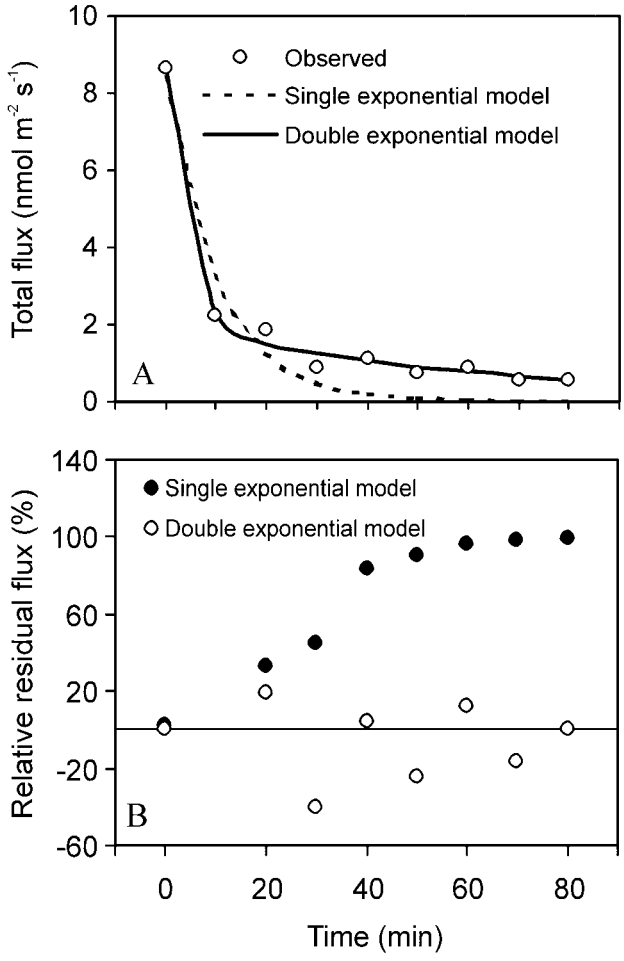

Figure 1. Fitting of time-dependent changes in monoterpene emission rate (F) after cuvette darkening at time t = 0 min in *Q. ilex* (data of *Loreto et al.* [1996a]). The data were fitted by single- and double-exponential models in **A**, and relative model residuals are depicted in **B**. The single-exponential model fits the emission data as $F = S_0 k e^{-kt}$, where S_0 is the initial pool size and k the rate constant. The double-exponential model is given as $F = S_0[\eta k_1 e^{-k_1 t} + (1-\eta)k_2 e^{-k_2 t}]$, where k_1 and k_2 are the time constants and η is the initial fraction of monoterpenoid present in the "faster" pool. The initial monoterpene content was found as the sum of all monoterpenoids emitted. The fraction of explained variance (r^2) was 0.77 for the single-exponential and r^2 = 0.994 for the double-exponential decay model.

2. Materials and Methods

2.1. Development of a Dynamic Monoterpene Emission Model

[9] Despite the conclusive evidence of foliar monoterpenoid storage in Mediterranean evergreen *Quercus* species, information of possible location of the storage pool is currently limited. However, determination of exact diffusion pathway as well as the surface area available for diffusion from the storage pool is critical to reliably simulate the dynamic responses of emission to changes in monoterpenoid synthesis rate. Therefore, we first develop a phenomenological model that allows quantitative description of the fluxes, and further relate the empirical time-constants of the model to theoretical diffusion pathway lengths in various leaf compartments, thereby allowing tentative estimation of the sites of storage.

[10] To estimate whether the stored compounds originate from a single pool or whether they diffuse from several pools of differing turnover time, we fitted monoterpene release data of darkened leaves of terpene-emitting species *Q. ilex* [*Loreto et al.*, 1996a, 1996c] and terpene-fumigated nonemitting species *Q. suber* [*Delfine et al.*, 2000] by exponential equations. All monoterpenoids emitted by *Q. suber* originate from a nonspecific storage, and we also

assume that no *de novo* monoterpenoid synthesis occurs in the darkened leaves of *Q. ilex* (s. Discussion for possible effects of monoterpenoid synthesis in the dark on predicted fluxes). All these experiments [*Loreto et al.*, 1996a, 1996c, 2000; *Delfine et al.*, 2000; *Niinemets et al.*, 2002a] demonstrated nonlinear decreases in monoterpenoid emission rates after darkening (*Q. ilex*, Figure 1a) and after cessation of terpene-fumigation (*Q. suber*). We expected that a single-exponential relationship would explain the time-dependent emission changes if the monoterpenoids are emitted from one storage pool only, and that a series of exponentials are necessary to fit the data if the emission originates from several pools.

[11] Fitting of the emission time-courses by a single-exponential decay model generally provided poor correspondence with the data (Figure 1a), and the lack of fit became larger with a time-dependent systematic error (Figure 1b), indicating that the monoterpenoids are likely stored in more than one pool. In contrast, double-exponential decay model resulted in a good agreement between the measured and observed monoterpene efflux estimates (Figure 1), suggesting that there are at least two storage pools of monoterpenoids with differing time constant. Given that application of a triple-exponential decay model nonsignificantly improved the fit (data not shown), we consider the double-exponential decay model appropriate.

[12] Thus, we apply a phenomenological model (Figure 2), which assumes that after production the monoterpenes can be stored in two abstract pools, one with a fast (first order rate constant k_1 [s^{-1}]) and another with a slow (k_2) turnover rate. The emission rate of each monoterpene from the pools, F, at time t is proportional to the storage pool size (S_1 [nmol m^{-2}] for the "fast" and S_2 [nmol m^{-2}] for the "slow" pool):

$$F(t) = k_1 S_1(t) + k_2 S_2(t) \tag{1}$$

The dynamics of both pools can be described as difference between monoterpene synthesis rate and efflux from the pools:

$$\frac{dS_1(t)}{dt} = \eta I - k_1 S_1(t) \tag{2a}$$

$$\frac{dS_2(t)}{dt} = (1-\eta) I - k_2 S_2(t), \tag{2b}$$

where I is the monoterpene production rate per leaf area [nmol m^{-2} s^{-1}], and η is a dimensionless coefficient determining the partitioning of synthesized monoterpenes between the pools. The rate of monoterpene production, I, may be calculated either by an empirical model that is driven by incident irradiance and leaf temperature [*Guenther et al.*, 1993; *Bertin et al.*, 1997; *Ciccioli et al.*, 1997] or may be determined from a correlation between monoterpene synthesis rate and the rate of photosynthetic electron transport [*Niinemets et al.*, 1999, 2002c], or the rate of photosynthesis [*Martin et al.*, 2000] (M. Reichstein et al., Canopy monoterpene emissions from an evergreen Mediterranean *Quercus ilex* forest: A test of three different models, submitted to *Journal of Geophysical Research*, 2002, hereinafter referred to as Reichstein et al., submitted manuscript, 2002).

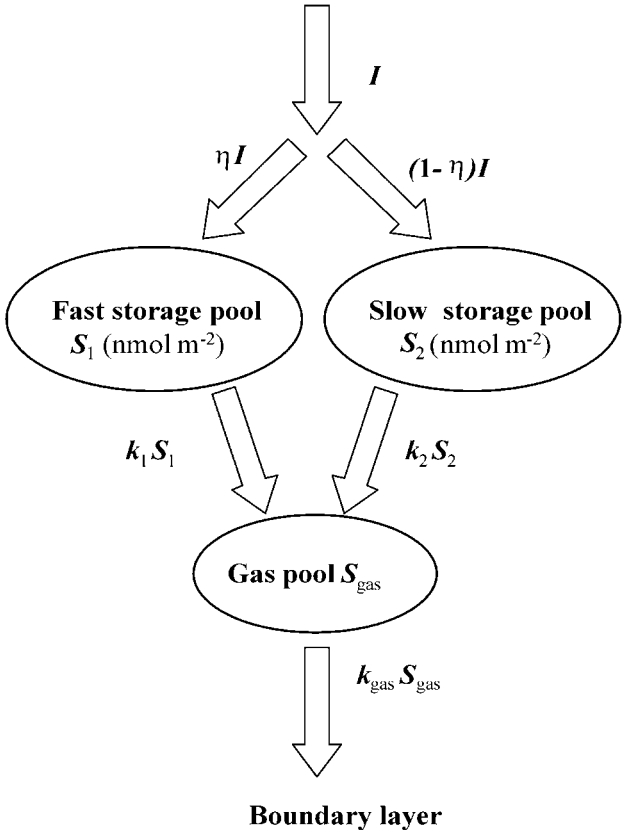

Figure 2. Outline of the dynamic model for simulation of nonspecific storage effects on foliar monoterpenoid emission in Mediterranean *Quercus* species. In the model, the monoterpenoids synthesized with a rate I are partitioned between two parallel storage pools of different time constant (k_1 and k_2) and size (S_1 and S_2). The monoterpenoids are emitted through the stomata with a rate $k_{gas}S_{gas}$, where k_{gas} is the stomatal rate constant and S_{gas} the gas-phase pool size.

[13] Integrating the system of differential equations (2a) and (2b) gives:

$$S_1(t) = \left(S_1(t_0) - \frac{\eta I}{k_1}\right) e^{-k_1 t} + \frac{\eta I}{k_1} \tag{3a}$$

$$S_2(t) = \left(S_2(t_0) - \frac{(1-\eta) I}{k_2}\right) e^{-k_2 t} + \frac{(1-\eta) I}{k_2}, \tag{3b}$$

where $S_1(t_0)$ and $S_2(t_0)$ are initial pool sizes. The half-times (τ) of the pools are given by $\tau = \ln(2)/k$, where k is the time-constant for the specific pool. In the steady state, $dS_1/dt = 0$ and $dS_2/dt = 0$, and the steady-state pool sizes are equal to:

$$S_1 = \frac{\eta I}{k_1} \tag{4a}$$

$$S_2 = \frac{(1-\eta) I}{k_2}. \tag{4b}$$

[14] We apply the model separately for each monoterpene, and find the total monoterpenoid emission rate as the sum of all individual monoterpenoid emission rates. The kinetic constants k_1 and k_2, and the fractional distribution of

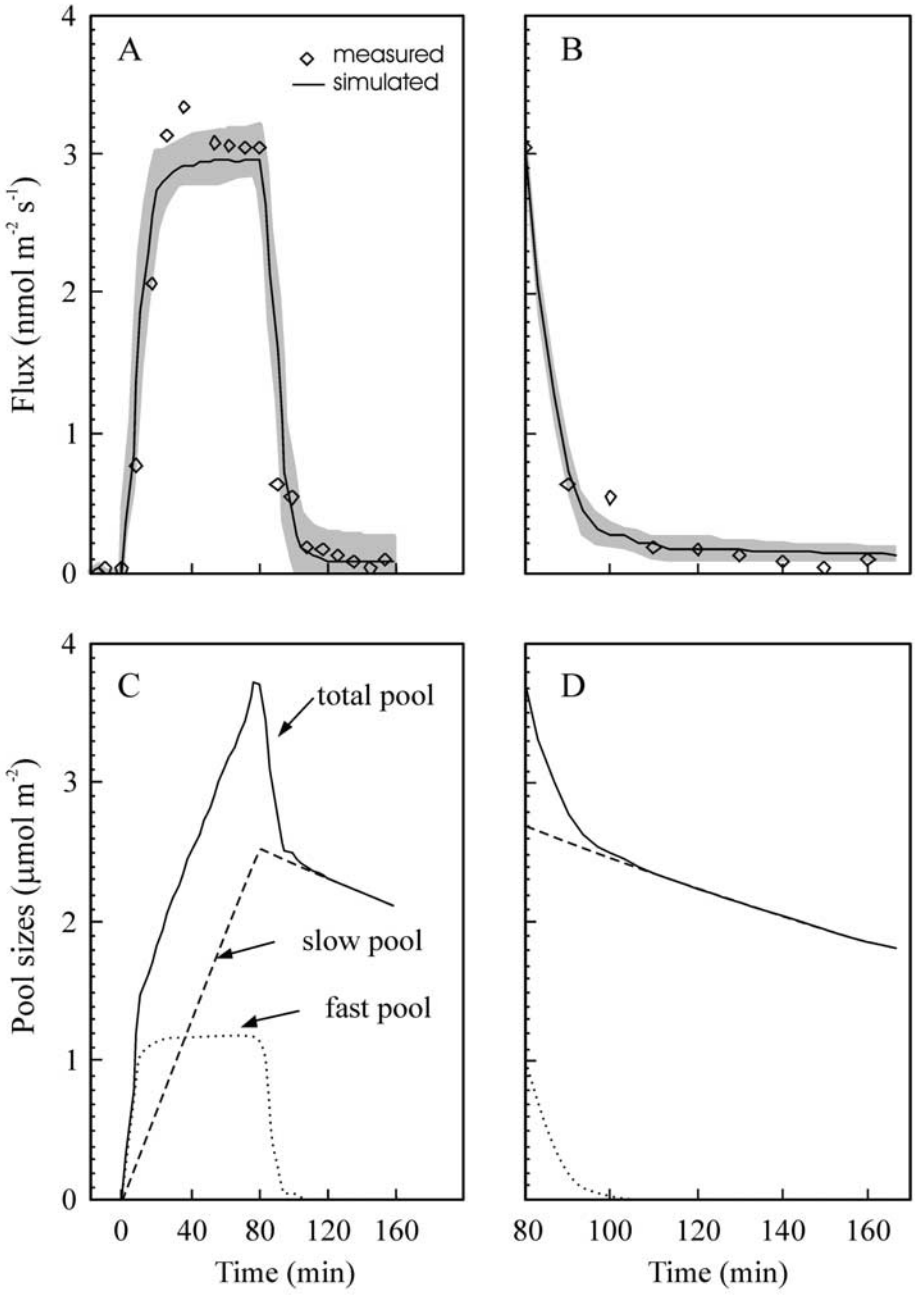

Figure 3. Measured (symbols, *Loreto et al.* [1996a]) and simulated (lines) time-courses of α-pinene emission rates (**A**, **B**) and estimated pool sizes of "slow", "fast" and total α-pinene storage pools (**C**, **D**). The light was switched on at $t = 0$ min and off at $t = 80$ min, and the model was fitted to the entire time-series (**A**, **C**) or only to the terpene efflux data after leaf darkening (**B**, **D**). The shaded areas in **A** and **B** give the 95% confidence intervals for the nonlinear fits [*Draper and Smith*, 1981].

synthesized monoterpenoid between the two pools, η, were determined for each monoterpenoid emitted by nonlinear fits to the emission decay data of *Q. ilex* [*Loreto et al.*, 1996a] and *Q. suber* [*Delfine et al.*, 2000] using the least sum of error squares criterion with Levenberg-Marquardt algorithm [*Draper and Smith*, 1981; *Visual Numerics*, 1993]. In *Q. ilex*, we also derived the model parameters using the entire emission time-course from the start of leaf illumination until the experiment termination (Figure 3). In these calculations, an estimate of the rate of monoterpene synthesis, I, was found as the average of four highest measurements by *Loreto et al.* [1996a].

2.2. Scaling of the Dynamic Model to Canopy Level and Comparison With Steady-State Approaches

[15] The phenomenological model (equations (1)– (3)) was employed to calculate the whole-canopy fluxes of monoterpenoids for a representative period in June 1997 in

Castelporziano, Rome, Italy (41°45′N, 12°22′E) in a mixed *Q. ilex*/*Pinus pinea* forest [*Valentini et al.*, 1992; *Manes et al.*, 1997] where extensive measurements of whole-canopy monoterpenoid emission fluxes have been carried out using a relaxed eddy-accumulation technique [*Moncrieff et al.*, 1997] (Reichstein et al., submitted manuscript, 2002). The rate of monoterpenoid synthesis in these simulations was computed for actual meteorological conditions with an emission model that employs a correlation between photosynthetic electron transport and monoterpenoid emission rate to describe the control of emission rates by incident quantum flux density, and the temperature dependence of the activity of monoterpenoid synthase to model the temperature effects on emission (ETR-model [*Niinemets et al.*, 2002c]). In this model, the empirical light dependence of monoterpene emission at a certain temperature is substituted by that of photosynthetic electron transport rate, assuming that monoterpene synthase is fully active in the leaves. Accordingly, the fraction of electrons going into monoterpene synthesis pathway depends on monoterpene synthase content of the leaves, and is basically equivalent with the emission rate in standardized conditions, E_S, used in other models [*Guenther et al.*, 1993, 2000; *Bertin et al.*, 1997]. The leaf-level model was scaled up to the stand level as detailed by (Reichstein et al. (submitted manuscript, 2002).

[16] For comparison, canopy monoterpenoid fluxes were also computed by the ETR-model and the Guenther et al. model [*Guenther et al.*, 1993, 2000] assuming that the synthesized monoterpenoids are immediately emitted. The Guenther et al. model [*Guenther et al.*, 1993, 2000] scales F_S to different leaf temperatures and incident quantum flux densities using empirical light and temperature correction functions. We have previously demonstrated (Reichstein et al., submitted manuscript, 2002) that for nonreactive atmospheric conditions both ETR and Guenther et al. model can be employed to reliably simulate whole canopy monoterpene emissions with the explained variances (r^2) between the simulated and measured canopy fluxes varying from 0.80 to 0.86 for different models. Our simulations also indicated that the ETR-model lacking a storage term predicts a larger sensitivity of canopy emission fluxes to environmental stresses (Reichstein et al., submitted manuscript, 2002).

2.3. Linking Storage Phenomena to Monoterpene Physico-Chemical Characteristics: A Flow/Conductance Model of Monoterpene Emission

[17] To gain insight into possible location of the storage pools, we first describe the monoterpene emission by a flow/conductance model, and further associate the measured kinetic constants of the pools with the conductances of the diffusion pathway.

[18] Although the cuticle may be permeable to monoterpenes [*Schmid et al.*, 1992], in *Q. ilex*, the monoterpenes are almost exclusively emitted by lower leaf side, where the stomata are located in this species [*Loreto et al.*, 1996c]. Because the cuticular emissions (0.009 nmol m^{-2} s^{-1} for α-pinene) are ca. three orders of magnitude less than the stomatal emissions (4.552 nmol m^{-2} s^{-1} [*Loreto et al.*, 1996c]), we neglect the cuticular conductance for monoterpenoids, and use an expression analogous to that previously employed to describe CO_2 diffusion into the leaf [*Farquhar and Sharkey*, 1982; *Ball*, 1987; *Field et al.*, 1989; see also *Tingey et al.*, 1991] for simulation of terpene efflux (F, mol m^{-2} s^{-1}):

$$F = \frac{D_A G_S (P_i - P_a)}{D_v P} + E\left(\frac{P_i - P_a}{2P}\right) \quad (5)$$

where D_A (m^2 s^{-1}, Appendix A, Table 1) is the air-phase diffusion coefficient for a specific monoterpene and D_v (m^2 s^{-1}) that for water vapor, G_S (mol m^{-2} s^{-1}) is the stomatal conductance for water vapor, P_i (Pa) is the terpene partial pressure in the substomatal cavities, and P_a (Pa) in the air, P (Pa) is the total air pressure and E (mol m^{-2} s^{-1}) leaf transpiration rate. The first part of this equation describes the control of terpene flux by stomata, the second part of the flux equation is attributable to mass flow due to net water flux through the stomata. Because the second part of the equation (5) is generally $\ll$ than the first part, we neglect the contribution of mass flow. Considering further that in well-mixed air no terpene build-up occurs in the leaf boundary layer and in the ambient air, P_a is practically zero under natural conditions. Thus, the intercellular terpene partial pressure is given as:

$$P_i = \frac{F D_v P}{D_A G_S}. \quad (6)$$

Analogously to CO_2 uptake by leaves [*Laisk and Oja*, 1998], we express the monoterpene diffusion flux from the site of synthesis in chloroplasts to substomatal cavities as:

$$F = G_M (C_w - P_i/H) \quad (7)$$

where G_M (m s^{-1}) is the monoterpene transfer conductance from chloroplasts to substomatal cavities, C_w (mol m^{-3}) is the water-phase monoterpene concentration in the chloroplast, and H (Pa m^3 mol^{-1}), the equilibrium air-water partition coefficient (Henry's law constant), converts the partial pressures to equivalent concentrations in the leaf liquid phase. For dilute aqueous solutions, H is equal to [*Staudinger and Roberts*, 1996]:

$$H = \frac{P_T}{C_a} = \frac{P_V}{\delta}, \quad (8)$$

where C_a (mol m^{-3}) is the liquid-phase monoterpene concentration at a monoterpene partial pressure of P_T, δ is the monoterpene solubility in water (mol m^{-3}) and P_V the saturating monoterpene partial pressure at a given temperature (Appendix A, Table 1). Aqueous solutions with less than 0.001 to 0.01 mole fraction of solute are considered dilute [*Staudinger and Roberts*, 1996]. Given that the solubility of all plant monoterpenoids is less than this threshold range (Table 1), we conclude that application of equation (8) is appropriate for plant monoterpenoids. We also assume that the aqueous mixtures of monoterpenoids are ideal, i.e., that the solubility of a specific monoterpenoid is unaffected by the presence of other monoterpenoids. This assumption has previously been verified for structurally similar hydrophobic compounds [*Banerjee*, 1984].

[19] Total mesophyll conductance consists of a liquid-phase conductance from the site of synthesis or storage, g_L (m s^{-1}), and a gas-phase conductance from the outer surface

Table 1. Physico-Chemical Properties of Monoterpenoids Emitted by *Q. ilex* at 25°C

Compound	P_V, Pa[a]	δ, mol m^{-3}	H, Pa m^3 mol^{-1}	$K_{o/w}$, mol mol^{-1}	D_A, m^2 s^{-1}	D_W, m^2 s^{-1}	g_{ias}, m s^{-1}	g_L, m s^{-1}
Camphor	9.87	8.12	1.22	219	$5.549 \cdot 10^{-6}$	$6.904 \cdot 10^{-10}$	$5.244 \cdot 10^{-3}$	$3.482 \cdot 10^{-4}$
Camphene	136	0.0849	1600	28,510	$5.842 \cdot 10^{-6}$	$7.007 \cdot 10^{-10}$	$5.520 \cdot 10^{-3}$	$2.145 \cdot 10^{-3}$
3-Carene	292	0.0214	13,640	40,740	$5.735 \cdot 10^{-6}$	$6.946 \cdot 10^{-10}$	$5.419 \cdot 10^{-3}$	$2.145 \cdot 10^{-3}$
1,8-Cineole	253	19.1	13.6	403	$5.456 \cdot 10^{-6}$	$6.640 \cdot 10^{-10}$	$5.156 \cdot 10^{-3}$	$5.261 \cdot 10^{-4}$
p-Cymene	197	0.179	1100	31,620[b]	$5.750 \cdot 10^{-6}$	$6.977 \cdot 10^{-10}$	$5.434 \cdot 10^{-3}$	$2.030 \cdot 10^{-3}$
Limonene	253	0.0886	2850	30,550	$5.645 \cdot 10^{-6}$	$6.817 \cdot 10^{-10}$	$5.334 \cdot 10^{-3}$	$2.081 \cdot 10^{-3}$
Linalool	21.3	10.2	2.09	933	$5.175 \cdot 10^{-6}$	$6.262 \cdot 10^{-10}$	$4.890 \cdot 10^{-3}$	$8.594 \cdot 10^{-4}$
Myrcene	265	0.0421	6300	21,630	$5.485 \cdot 10^{-6}$	$6.522 \cdot 10^{-10}$	$5.183 \cdot 10^{-3}$	$1.957 \cdot 10^{-3}$
cis-β-Ocimene	197	0.0797	2470	23,530	$5.463 \cdot 10^{-6}$	$6.522 \cdot 10^{-10}$	$5.162 \cdot 10^{-3}$	$1.968 \cdot 10^{-3}$
trans-β-Ocimene	197[c]	0.0592	3330	28,200	$5.463 \cdot 10^{-6}$	$6.522 \cdot 10^{-10}$	$5.162 \cdot 10^{-3}$	$1.987 \cdot 10^{-3}$
α-Phellandrene	198	0.0285	6950	38,460	$5.651 \cdot 10^{-6}$	$6.817 \cdot 10^{-10}$	$5.340 \cdot 10^{-3}$	$2.102 \cdot 10^{-3}$
β-Phellandrene	204	0.036	5670	38,160	$5.654 \cdot 10^{-6}$	$6.817 \cdot 10^{-10}$	$5.343 \cdot 10^{-3}$	$2.095 \cdot 10^{-3}$
α-Pinene	558	0.0411	13,600	30,900	$5.812 \cdot 10^{-6}$	$7.001 \cdot 10^{-10}$	$5.493 \cdot 10^{-3}$	$2.135 \cdot 10^{-3}$
β-Pinene	404	0.0592	6830	26,300	$5.786 \cdot 10^{-6}$	$7.001 \cdot 10^{-10}$	$5.468 \cdot 10^{-3}$	$2.116 \cdot 10^{-3}$
Sabinene	342	0.053	6450	42,660	$5.756 \cdot 10^{-6}$	$6.946 \cdot 10^{-10}$	$5.440 \cdot 10^{-3}$	$2.149 \cdot 10^{-3}$
α-Terpinene	202	0.103	1960	5060	$5.648 \cdot 10^{-6}$	$6.817 \cdot 10^{-10}$	$5.337 \cdot 10^{-3}$	$1.697 \cdot 10^{-3}$
γ-Terpinene	146	0.0562	3590	31,620	$5.627 \cdot 10^{-6}$	$6.817 \cdot 10^{-10}$	$5.318 \cdot 10^{-3}$	$2.084 \cdot 10^{-3}$
α-Terpineol	3.07	12.6	0.239	955	$5.290 \cdot 10^{-6}$	$6.526 \cdot 10^{-10}$	$4.999 \cdot 10^{-3}$	$8.851 \cdot 10^{-4}$
α-Terpinolene	79.1	0.0404	2600	29,510	$5.622 \cdot 10^{-6}$	$6.817 \cdot 10^{-10}$	$5.313 \cdot 10^{-3}$	$2.077 \cdot 10^{-3}$

Q. ilex emits at least 22 different monoterpenoids [*Loreto et al.*, 1998; *Staudt et al.*, 2001; *Niinemets et al.*, 2002c]. Tricyclene and α-thujene were excluded because of limited physico-chemical data.

[a] P_V = saturated vapor pressure (calculated according to equations (A5) and (A6)); δ = water solubility; H = Henry's law constant (calculated as P_V/δ); $K_{o/w}$ = octanol/water partition coefficient; D_A = binary diffusion coefficient in air (equation (A1)); D_W = diffusion coefficient in water (equation (A2)); g_{ias} = intercellular gas-phase conductance from outer surface of cell walls to substomatal cavities (equation (16)); g_L = liquid-phase diffusion conductance from the site of synthesis to outer surface of cell walls (equation (17)). In these calculations, the site of diffusion was assumed to be in the chloroplasts of mesophyll cells for all compounds. The leaf anatomical variables of *Q. ilex* used in calculations of g_{ias} and g_L are given in Table 2. Data sources of all monoterpenoid physico-chemical characteristics are provided in Appendix A.

[b] An estimate for *m*-cymene.

[c] The value for *cis*-β-ocimene.

of cell walls to substomatal cavities g_{ias} (m s^{-1}) [*Evans et al.*, 1994; *Parkhurst*, 1994; *Syvertsen et al.*, 1995]. G_M is a liquid-phase conductance, and is given as the inverse of the sum of the component serial resistances [*Thomas*, 1990; *Evans et al.*, 1994]:

$$\frac{1}{G_M} = \left(\frac{1}{g_L} + \frac{RT}{Hg_{ias}}\right), \tag{9}$$

where R is the gas constant (8.314 J mol^{-1} K^{-1}), and T leaf temperature (K). The ratio $H/(RT)$ gives the dimensionless Henry's law constant, and converts the gas-phase conductance to a liquid-phase equivalent conductance [*Mackay and Shiu*, 1981; *Thomas*, 1990; *Laisk and Oja*, 1998].

2.4. Theoretical Determination of the Kinetic Constants of the Model

[20] We have previously demonstrated that the half-time of the gas-phase pool (τ_G, Figure 2) of monoterpenoids with a high value of Henry's law constant ($H > \sim$100 Pa m^3 mol^{-1}) is on the order of 0.1–0.5 s in a situation with open stomata, and τ_G is on the order of few seconds when the stomata are closed [*Niinemets et al.*, 2002b]. Given further that the half-times for stomatal opening are on the order of minutes [*Tinoco-Ojanguren and Pearcy*, 1993], the gas-phase pool of monoterpenes with a large H is always essentially in a steady state [*Niinemets et al.*, 2002b]. The experimental fitting of terpene emission decay data (Figure 1) also provided half-times of the monoterpene storage pools that are $\gg\tau_G$. The H values are relatively low for camphor, 1,8-cineole, linalool and α-terpineol (Table 1), but these monoterpenoids are emitted only in trace quantities in *Q. ilex* [*Niinemets et al.*, 2002c]. Given that the major monoterpenoids of *Q. ilex* have $H > 1000$ Pa m^3 mol^{-1} (Table 1), we conclude that the monoterpene storage pool cannot be in the gas phase. However, the monoterpenoid storage may be either in the leaf liquid or lipid phase.

[21] Let us first assume that the storage pools are in the liquid phase. Thus, the size of the storage pool S_j is related to monoterpene mesophyll concentration $C_{w,j}$ as:

$$S_j = C_{w,j}\frac{f_{w,j}V}{A}, \tag{10}$$

where V (m^3) is leaf volume and A is projected leaf surface area (m^2), and $f_{w,j}$ is the volumetric leaf water fraction attributable to pool S_j. Thus, we can relate the rate constant k_j to mesophyll conductance:

$$F_j = k_j S_j = k_j C_{w,j}\frac{f_{w,j}V}{A} = G_{M,j}\left(C_{w,j} - P_i/H\right). \tag{11}$$

Combining equation (11) with equation (9) and assuming that $P_i/H \ll C_{w,j}$ we get:

$$k_j = G_{M,j}\frac{A}{f_{w,j}V} = \frac{A}{f_{w,j}V}\left(\frac{g_{L,j}H}{H + \frac{RTg_{L,j}}{g_{ias,j}}}\right). \tag{12}$$

This equation predicts that whenever the storage pool is located in the liquid phase, k_j is hyperbolically related to the Henry's law constant of the considered monoterpene. Given that the liquid-phase conductance, g_L, is a composite conductance as outlined below, total mesophyll conductance of the specific monoterpenoid may be calculated depending on the location of the storage pool, e.g., cell wall

versus chloroplasts. To test the assumption that P_i/H may be neglected in equation (12), we determined P_i by equation (6) for various monoterpenoids from the data of *Loreto et al.* [1998], and partitioned the measured total monoterpenoid pool between pools S_1 and S_2 using the parameterized dynamic monoterpenoid emission model (equations (2) and equations (3), see section 3). The ratio $P_i/(C_{w,j}H)$ was less than 10^{-3} for all monoterpenoids with a large Henry's law constant ($H > 10^3$ Pa m^3 mol^{-1}, Table 1), suggesting that P_i/H ratio may generally be discarded. However, for linalool with a low value of H (Table 1), this ratio was 0.10, indicating that the gas-phase conductance for monoterpenoids with a low H may partly control the kinetics of monoterpenoid efflux from the leaves [see also *Niinemets et al.*, 2002b].

[22] Analogously, the diffusion equations may be formulated for monoterpene efflux from the leaf lipid pool. In this case, the pool size is given by:

$$S_j = C_{L,j}\frac{f_{L,j}V}{A}, \tag{13}$$

where $C_{L,j}$ (mol m^{-3}) is the monoterpenoid lipid-phase concentration in pool S_j, and $f_{L,j}$ is the lipid volume fraction of the specific pool. Monoterpene efflux from the lipid phase to substomatal cavities is described as:

$$F_j = k_j S_j = k_j C_{L,j}\frac{f_{L,j}V}{A} = G_{L,j}\left(C_{L,j} - P_i/K_{A/L}\right), \tag{14}$$

where $K_{A/L}$ (Pa m^3 mol^{-1}) is the air- to lipid-phase distribution coefficient, $f_{L,j}$ is the lipid volume fraction in the leaf (m^3 m^{-3}), and $G_{L,j}$ (m s^{-1}) is the diffusion conductance from the lipid phase to substomatal cavities. We computed an estimate of $K_{A/L}$ as the ratio of H (equation (8)) to monoterpenoid octanol/water partition coefficient ($K_{o/w}$, Table 1). There is evidence that $K_{o/w}$ is not only strongly correlated with lipid- to water-phase partitioning coefficients, but also that the magnitude of $K_{o/w}$ matches that of the lipid to water partition coefficient. For example, the cuticle to water partition coefficient of several monoterpenoids was on average only 0.77 ± 0.06 times lower than corresponding $K_{o/w}$ [*Schmid et al.*, 1992], suggesting that $K_{o/w}$ may correctly estimate leaf lipid to water partition coefficients (but see Discussion).

[23] P_i/H ratio in equation (11), $P_i/K_{A/L}$ ratio cannot generally be discarded, because $K_{A/L}$ is five orders of magnitude smaller than H, demonstrating that even small monoterpenoid intercellular partial pressures may alter the effective diffusion gradient from lipids to ambient air. Thus, whenever the storage pool is in the lipid phase, the rate constant of the pool is given as:

$$k_j = \frac{G_{L,j}A}{f_{L,j}V}\left(1 - \frac{P_i}{C_{L,j}K_{A/L}}\right). \tag{15}$$

This equation indicates that for the monoterpene efflux from the lipid phase, the rate constant should be inversely proportional to monoterpenoid air/lipid-phase distribution coefficient. The estimates of $P_i/(C_{L,j}K_{A/L})$ for various monoterpenoids were determined from *Loreto et al.* [1998] after partitioning of the total leaf monoterpenoid pool size between the component pools by the dynamic emission model (equations (1)–(3)).

2.5. Estimation of Mesophyll Diffusion Conductances for Gas and Liquid Phases

[24] The gas-phase monoterpenoid conductance is dependent on the fraction of intercellular air space (f_{ias}, m^3 m^{-3} [*Syvertsen et al.*, 1995; *Terashima et al.*, 1995]) and the monoterpenoid diffusion coefficient in the air (D_A) as:

$$g_{ias} = \frac{D_A f_{ias}}{\Delta L_{ias}\varsigma}, \tag{16}$$

where ΔL_{ias} is the diffusion path length (m) in the gas phase, and ς the diffusion path tortuosity (m m^{-1}). Half of leaf thickness was used for ΔL_{ias} (Table 2), and an estimate of 1.57 m m^{-1} for ς. The latter value is an average determined from measurements of leaf thickness and CO_2 mesophyll conductance in four woody thick-leaved species [*Syvertsen et al.*, 1995]. This path length tortuosity is in a good agreement with anatomical measurements from leaf paradermal and transverse sections, that provided an average value for 8 species of 1.36 m m^{-1} [*Terashima et al.*, 1995]. f_{ias} was determined using available data on the size of mesophyll cells, and fraction of mesophyll in leaf cross-section. The shape of palisade and spongy mesophyll cells was approximated by a prolate spheroid in cell volume calculations (Table 2).

[25] The liquid-phase pathway consists of cell wall, plasmalemma, cytosol, chloroplast envelope and chloroplast stroma, and the total conductance may be expressed as the inverse of the sum of the component serial resistances:

$$\frac{1}{g_L} = \frac{A}{A_{mes}}\left(\frac{1}{g_{cw}} + \frac{1}{g_{pl}} + \frac{1}{g_{ct}} + \frac{1}{g_{en}} + \frac{1}{g_{st}}\right), \tag{17}$$

where g_{cw} is the cell wall, g_{pl} the plasmalemma, g_{ct} the cytosol, g_{en} the chloroplast envelope, and g_{st} the chloroplast stroma conductance to monoterpene considered, and the ratio of mesophyll surface (A_{mes}) to projected leaf surface area (A) corrects for the actual area available for diffusion [*Nobel*, 1991]. Implicit in the use of A_{mes}/A ratio to scale the conductances is the assumption that the cell wall, plasmalemma, and chloroplast exposed surface areas are essentially the same [*Nobel*, 1991]. A_{mes}/A ratio was computed according to *Nobel* [1991], using the available sizes of palisade and spongy mesophyll cells, and approximating the cell shape to a prolate spheroid. A_{mes}/A calculations were corrected for the fraction of air space in the leaves. The cell wall, cytosol and stroma conductances were calculated as [cf. *Tingey et al.*, 1991; *Nobel*, 1991, equation (8.19)]:

$$g_i = \frac{r_f D_W p}{\Delta L_i}, \tag{18}$$

where g_i (m s^{-1}) is either g_{cw}, g_{ct} or g_{st}, D_W (m^2 s^{-1}) is the aqueous-phase monoterpene diffusion coefficient (Appendix A), ΔL_i (m) is the diffusion path length, and p (m^3 m^{-3}) is the effective porosity. Dimensionless coefficient r_f accounts for the decrease of the diffusion conductance because of greater water viscosity and path length tortuosity in cytosol and in chloroplast stroma (r_f = 1 for cell wall) than in pure

Table 2. Leaf-Dependent Characteristics Used in Simulations With *Q. ilex*

Characteristic	Symbol (unit)	Value [Reference][a]
Leaf surface area (A) to volume ratio (V)	A/V (m^2 m^{-3})	3910 [*Christodoulakis and Mitrakos*, 1987; *Terradas and Savé*, 1992; *Wagner et al.*, 1993; *Castro-Díez et al.*, 1997; *Tretiach et al.*, 1997; *Grossoni et al.*, 1998]
Leaf dry mass per unit area	M_A (g m^{-2})	181 [*Christodoulakis and Mitrakos*, 1987; *Terradas and Savé*, 1992; *Wagner et al.*, 1993; *Castro-Díez et al.*, 1997; *Grossoni et al.*, 1998]
Fraction of intercellular air space within the leaf	f_{ias} (m^3 m^{-3})	0.181 [*Wagner et al.*, 1993]*2
Volumetric foliar water fraction	f_w (m^3 m^{-3})	0.491 [*Gratani and Fiorentino*, 1988; *Gratani et al.*, 1989; *Gratani*, 1995]
Volumetric foliar lipid fraction[b]	f_L (m^3 m^{-3})	0.029 [*Diamantoglou and Kull*, 1982]
Effective diffusion path length in the gas phase	ΔL_{ias} (m)	$1.22 \cdot 10^{-4}$ [*Christodoulakis and Mitrakos*, 1987; *Terradas and Savé*, 1992; *Wagner et al.*, 1993; *Castro-Díez et al.*, 1997; *Grossoni et al.*, 1998]
Exposed mesophyll area to A ratio	A_{mes}/A (m^2 m^{-2})	30.5 [*Wagner et al.*, 1993]
Diffusion path length in the cell wall	ΔL_{cw} (m)	$5.0 \cdot 10^{-7}$ [*Grossoni et al.*, 1998; *Paoletti*, 1998]
Diffusion path length in the cytosol	ΔL_{ct} (m)	$9.7 \cdot 10^{-8}$ [*Paoletti*, 1998]
Diffusion path length in the chloroplast stroma[c]	ΔL_{st} (m)	$1.65 \cdot 10^{-6}$ [*Paoletti*, 1998]

[a] An average value was calculated for variables with multiple estimates.
[b] Calculated from measurements in *Q. coccifera*, and assuming that lipid density is 0.9 g cm^{-3} [*Büscher*, 1960].
[c] Half of the chloroplast side-length perpendicular to the cell-wall.

water [*Weisiger*, 1998]. An estimate of r_f of 0.294 for g_{ct} and g_{st} was obtained as the ratio of effective water self-diffusion coefficients in duck embryo and in chemically pure water [*Weisiger*, 1998]. Effective porosity, p, was taken as 1 for g_{ct} or g_{st} and 0.3 for cell walls. These are typical values for CO_2 liquid-phase diffusion [*Nobel*, 1991; *Evans et al.*, 1994; *Parkhurst*, 1994], but may be lower for larger molecules. In fact, the actual diffusion path tortuosity in the gas phase is likely larger for monoterpenoids with larger diffusion volume than that for CO_2 (equation (16)). The effective cell wall pore volume for monoterpenoids with an average molecular diameter of ca. 8 Å may also be less than that for CO_2 (~3 Å). In particular, due to a greater number of dead ends in the cell wall matrix. The largest pore diameters range from 35 to 52 Å in mesophyll cell walls [*Carpita et al.*, 1979], but average pore sizes may be significantly less. Furthermore, we consider the monoterpene diffusion in intercellular air space and in cell walls as simple diffusion though free air or water, but air-phase passages between the neighboring cells as well as the pore diameters within the cell walls may be sufficiently small to increase the diffusion limitations via Knudsen diffusion [*Leuning*, 1983; *Parkhurst*, 1994] that results from additional collisions of diffusing molecules with the walls of the passage. Because of lacking detailed geometrical information of internal leaf architecture, such effects cannot currently be quantified, but we suggest that the resulting overestimation of monoterpenoid gas- and liquid-phase diffusion conductances is likely less than an order of magnitude.

[26] The rate of simple diffusion across a cell membrane is limited by the movement of the molecule from the aqueous environment outside or inside the cell into the membrane lipid bilayer. Therefore, transport rates for specific compounds are proportional to the lipid solubilities of these compounds. Thus, plasmalemma permeability to monoterpenes may be expressed as:

$$g_{pl} = \frac{D_{pl} K_{pl/w}}{\Delta L_{pl}}, \quad (19)$$

where D_{pl} (m^2 s^{-1}) is the monoterpene diffusion coefficient in the plasmalemma, ΔL_i (m) is the plasmalemma thickness, and $K_{pl/w}$ is the monoterpene plasmalemma to water partition coefficient. $K_{pl/w}$ is the ratio of monoterpene concentration in the plasmalemma to the concentration in equilibrium outside in the water phase [*Nobel*, 1991]. Chloroplast envelope permeability, g_{en}, may be expressed in an analogous manner. For various monoterpenoids, we calculated g_{pl} and g_{en} from the correlation between experimentally determined permeabilities of mesophyll cell plasmalemma and chloroplast envelope [*Gimmler et al.*, 1981; *Daeter and Hartung*, 1993] versus the compound diffusion volume (V_M, cm^3 mol^{-1}, Appendix A) and octanol/water partition coefficients ($K_{o/w}$). Because the original studies reported estimates of g_{pl} and g_{en} in relation to octanol to assay medium partition coefficient ($K_{o/m}$), a correlation between literature estimates of $K_{o/w}$ and $K_{o/m}$ was used to compute g_{pl} and g_{en} from $K_{o/w}$:

$$g_{pl} = \frac{6.70 \cdot 10^{-4} K_{o/w}^{0.67}}{V_M^{0.918}}, \quad (20)$$

and

$$g_{en} = \frac{4.98 \cdot 10^{-5} K_{o/w}^{0.796}}{V_M^{0.543}} \quad (21)$$

($r^2 = 0.86$ for g_{pl} and $r^2 = 0.89$ for g_{en}). Data of *Gimmler et al.* [1981], and these equations predict that the permeability of chloroplast envelope is one to two orders of magnitude greater than that of the plasmalemma. However, it is unclear how these calculations account for the aquaporin conductance that may dramatically increase membrane permeability for water and other relatively small molecules [*Maurel*, 1997].

2.6. Lipid-Phase Diffusion Conductance

[27] The lipid-phase diffusion conductance from the lipid pool to substomatal cavities, G_L, depends on the monoterpenoid diffusion in the lipid phase, but also

involves the diffusion through aqueous and gas phases (equation (9)):

$$\frac{1}{G_L} = \frac{1}{\frac{A_{mes} D_L}{\Delta L_L A}} + \frac{K_{o/w}}{g_L} + \frac{K_{o/w} RT}{H g_{ias}}, \quad (22)$$

where D_L ($m^2\ s^{-1}$) is the effective monoterpenoid diffusion coefficient in the lipid phase, and ΔL_L the effective diffusion path length. The first part of equation (22) describes the monoterpene diffusion through the lipid phase, whereas the second and third components characterize the diffusion through aqueous and gas phases that separate the lipid pool from the substomatal cavities. Octanol/water partition coefficient converts the liquid-phase conductances to equivalent lipid-phase conductances. Like in equation (14), we assume that $K_{o/w}$ provides an estimate of monoterpenoid partitioning between leaf lipid and water fractions. Equation (22) essentially indicates that with increasing $K_{o/w}$, the effective monoterpenoid pool in the hydrophobic environment becomes larger.

[28] The length of the diffusion pathway through cell water (equation (17)) depends on the location of the lipid-phase storage pool. For example, if the monoterpenoids are stored in thylakoid membranes, the diffusion pathway includes all components of equation (17). For the cuticle, the aqueous-phase pathway may be through the cell walls only or may be entirely missing. In the following calculations we consider the longest aqueous-phase pathway, i.e., the monoterpenoid storage in the inner membranes of cell organelles.

[29] Although the information of monoterpenoid mobility in cell organelle membranes is not available, estimates of D_L may be obtained from plasmalemma and chloroplast envelope permeabilities and plasmalemma ($K_{pl/w}$) and chloroplast envelope ($K_{en/w}$) to water partition coefficients as $g_{pl}/K_{pl/w}$ and $g_{en}/K_{en/w}$ divided by half-membrane thickness (equation (19)). Again, monoterpenoid octanol to water partition coefficients were used as substitutes of $K_{pl/w}$ and $K_{en/w}$. Considering further that plasmalemma thickness is ca. 100 Å [*Falk and Stocking*, 1976] and the total thickness of two chloroplast envelope membranes ca. 140 Å [*Falk and Stocking*, 1976; *Heber and Heldt*, 1981], estimates of D_L range from $(2.1–2.6) \cdot 10^{-15}$ $m^2\ s^{-1}$ for the chloroplast membranes, and $(2.6–3) \cdot 10^{-16}$ $m^2\ s^{-1}$ for the plasmalemma.

[30] As an alternative assessment of lipid-phase mobility of various monoterpenoids, we determined the diffusion coefficient of monoterpenoids in the cuticle (D_C, $m^2\ s^{-1}$). For hydrophobic compounds D_C at 25°C is given as [*Schönherr and Baur*, 1994; *Schreiber et al.*, 1996]:

$$D_C = D_0 e^{-\beta V_S}, \quad (23)$$

where V_S is the Schroeder's molar volume [*Nelken*, 1990] calculated in a similar manner as V_M in equations (20)–(21), D_0 is the diffusion coefficient for a hypothetical molecule with $V_S = 0$, and the empirical parameter β (mol cm^{-3}) describes the sensitivity of D_C to V_M. Equation (23) was parameterized using experimental values of $D_C = 1.18 \cdot 10^{-14}$ $m^2\ s^{-1}$ for α-pinene and of $D_C = 4.65 \cdot 10^{-15}$ $m^2\ s^{-1}$ for limonene obtained for the cuticles of *Picea abies* [*Schmid*, 1991] (see also *Schmid et al.* [1992] for methods of cuticle isolation). A nonlinear fit of these data to equation (23) gave an estimate of $1.34 \cdot 10^{-9}$ $m^2\ s^{-1}$ for D_0 and 0.0665 mol cm^{-3} for β, and the corresponding D_C range of the monoterpenoids considered was $(0.074–1.18) \cdot 10^{-14}$ $m^2\ s^{-1}$. Measurements of D_C in the isolates cuticles of *Fagus sylvatica*, gave values of $D_0 = 6.22 \cdot 10^{-14}$ $m^2\ s^{-1}$ and $\beta = 0.036$ mol cm^{-3} for a set of compounds mainly consisting of a variety of long-chained aliphatic molecules, but including isoprenoids abscisic acid and cholesterol [*Schreiber et al.*, 1996]. The original parameterization of *Schreiber et al.* [1996] provides D_C values of $4.74 \cdot 10^{-16}$ $m^2\ s^{-1}$ for α-pinene and $3.37 \cdot 10^{-16}$ $m^2\ s^{-1}$ for limonene.

[31] The effective diffusion path length for the lipid phase may widely vary depending on the site of diffusion, extending from ca. 50–70 Å for the plasmalemma and envelope membranes of cell organelles to more than 2000 Å in stacked thylakoid membranes [*Weier et al.*, 1967] as well as in the cuticle. Although the thylakoid membranes in grana are separated by aqueous layers [*Weier et al.*, 1967], and the thickness of each membrane is on the order of 85–100 Å, the diffusion through the unstirred aqueous layers may often be the rate-limiting step in membrane diffusion, such that the effective diffusion path length through the membrane is considerably longer [*Nobel*, 1991]. We used a conservative estimate of 200 Å for ΔL_L, assuming that most of the terpene efflux from the lipid pool is associated with plasmalemma and chloroplast envelope membranes.

3. Results

3.1. Parameters of the Dynamic Monoterpene Emission Model

[32] In *Q. ilex*, fitting of dynamic emission patterns by two time constants provided generally good correspondence with the data (Figures 3a and 3b). Among various monoterpenoids, the time constant of the "fast" pool, k_1, was one to three orders of magnitude larger than the time-constant of the "slow" pool (equations (1)–(3)(3); Table 3). The time constants were not correlated ($r^2 = 0.01$, $P > 0.9$), suggesting that the two pools may be physically separated in the leaf. Although the time constants of the pools derived from the actual leaf emission measurements in *Q. ilex* (data of *Loreto et al.* [1996a]) differed somewhat from those determined using monoterpene efflux data in fumigated leaves of the nonemitting species *Q. suber* (data of *Delfine et al.* [2000]), various estimates of k_1 ($r^2 = 0.94$, $P < 0.03$ for the linear regression with the four monoterpenoids available in both studies), and k_2 ($r^2 = 0.80$, $P < 0.10$) were correlated. Thus, terpene efflux measurements from the fumigated leaves of a species not synthesizing monoterpenoids further confirm the suggestion that there are two nonspecific foliar monoterpenoid storage pools of varying kinetics.

[33] The half-time of the "fast" pool, τ_1, varied 3.5-fold for the nine monoterpenoids in *Q. ilex*, but the half-time of the "slow" pool, τ_2, varied more than 30-fold (Table 3). The fractional allocation of synthesized monoterpenoids to the "fast" pool, η, also varied, but only 1.4-fold.

[34] The significance of varying the time constants k_1 and k_2 as well as the allocation between various monoterpenoids is demonstrated in Figure 4. Modification of the decay kinetic of the "fast" pool may strongly affect the initial response of the emission rate to rapid changes in environmental variables,

Table 3. Half-Times of the "Fast" (τ_1) and "Slow" (τ_2) Storage Pools, the Fraction of Synthesized Monoterpenoids Going Into the "Fast" Storage Pool (η) and the Total Pool Size (S_T) in *Q. Ilex*[a]

Compound	τ_1, h	τ_2, h	η, mol mol^{-1}	S_T, nmol m^{-2}
p-Cymene	0.228	25.9	0.697	403
Myrcene	0.123	1.26	0.840	1195
cis-β-Ocimene	0.165	4.60	0.782	478
β-Phellandrene	0.146	32.9	0.762	252
α-Pinene	0.0783	5.70	0.867	2966
β-Pinene	0.0784	3.62	0.846	2284
Sabinene	0.0652	47.6	0.629	979
γ-Terpinene	0.138	7.96	0.811	394
α-Terpinolene	0.171	16.1	0.736	297
Total emission	0.0782	2.05	0.865	10,480[b]

[a] The dynamic monoterpenoid emission model (equations (1)–(3)) was parameterized using the measurements of *Loreto et al.* [1996a]. The data were fitted to the entire experiment, which included an 80-min leaf illumination period, followed by an 80-min dark period. Total storage pool size (S_T) was estimated by integrating the monoterpene fluxes after leaf darkening.

[b] In addition to the monoterpenoids depicted, five other monoterpenoids were emitted in significant quantities after leaf darkening [*Loreto et al.*, 1996a].

e.g., to changes in light intensity (Figures 4a and 4b). Dynamics of the "slow" pool primarily determines the time required for the flux to reach a steady state with a given monoterpenoid synthesis rate, but also affects the leaf response to more gradual changes in environmental variables (Figures 4c and 4d).

[35] Variation in η that determines the relative importance of the "fast" and "slow" pool dynamics has a major influence on the emission patterns (Figures 4e and 4f). Although η varied little between various monoterpenoids (Table 3), even such a limited variability may have dominant effects on the monoterpenoid emission dynamics.

3.2. Correspondence Between Estimated and Measured Storage Pool Sizes

[36] *Loreto et al.* [1998] provides estimates of monoterpenoid pool sizes after 60 min. of continuous leaf illumination. These pool sizes compare well with our model assessments calculated using the time constants of specific monoterpenoids (Figure 5a, Table 3), thereby providing an independent verification of our model.

[37] Because the system is far from being in a steady state, the exact time period is essential for the comparison. We observed the best correspondence (Figure 5a) with model estimates at $t = 30$ min. rather that at $t = 60$ min. used in the experiments of *Loreto et al.* [1998]. However, the total monoterpenoid emission rate in the study used for model parameterization [*Loreto et al.*, 1996a] was 9.4 nmol m^{-2} s^{-1}, but was 4.5 nmol m^{-2} s^{-1} by *Loreto et al.* [1998]. Therefore, we conclude that roughly two-fold larger pool size predicted by the model is attributable to study-to-study differences in the monoterpenoid synthesis rate (equation (2)).

[38] The correlation in Figure 5a is not only the outcome of differing monoterpenoid physico-chemical characteristics, but the storage pool size depends on the synthesis rate of specific monoterpenoid as well. Thus, species-specific activities of monoterpenoid synthases also control the pool sizes of various monoterpenoids. To distinguish between the monoterpene physico-chemical characteristics and inherent differences in the emission spectrum, we calculated the steady-state pool sizes for a constant monoterpenoid synthesis rate (Figure 5b). This plot demonstrates that the potential storage pool size is not related to the rate constant k_1, but is primarily governed by the rate constant k_2. Accordingly, the dynamics of the "slow" pool primarily influences the monoterpene emission from darkened leaves in a long term. The large steady-state pool sizes are in accord with measured monoterpenoid contents in *Q. ilex* leaves that were fumigated with high air concentrations of various monoterpenoids (Figure 5b) (data of *Delfine et al.* [2000]). Furthermore, leaf fumigation with monoterpenoids with constant air-phase mixing ratios yielded pool sizes that are in a good accordance with simulated steady-state values (Figure 5b), providing evidence that monoterpenoid physico-chemical characteristics strongly control the pool size.

3.3. Changes in the Fractional Composition of Emitted Monoterpenoids

[39] Apart from the progressive decline in terpene emission rates in darkened leaves and after termination of fumigation, the fractional composition of emitted monoterpenoids was also temporarily altered. The fractional contribution to total emission of monoterpenoids with a relatively high k_1 decreased (α-pinene in Figure 6), while that of compounds with lower k_1 (myrcene and *cis*-β-ocimene in Figure 6) increased, and that of compounds with intermediate k_1 was relatively constant (β-pinene in Figure 6). This temporal change of the composition of emitted monoterpenoids is consistent with differences in the decay kinetics of the "fast" pool.

[40] Simulations further demonstrated that modification of the fractional composition of the emitted monoterpenoids also occurs in response to rapid changes in environmental factors that alter the rate of monoterpenoid synthesis (I, Figure 7). Contrary to emission responses after cessation of monoterpenoid synthesis rate (Figure 6), rapid increases in monoterpenoid synthesis rate lead to a larger fraction of compounds with high k_1 (Figure 7b). This is because the steady-state flux rate is achieved faster (Figure 7a), and the same flux rate can be maintained with a lower pool size in these monoterpenoid species. Again, a rapid decline in the rate of monoterpene synthesis affected less strongly the compounds with a lower k_1 (*cis*-β-ocimene, myrcene), because the nonspecific storage pools accumulated during the period of a constant rate of synthesis were larger for these compounds (Figures 7c and 7d).

3.4. Scaling the Results to a Canopy Level

[41] A comparison of the dynamic model with the steady-state emission algorithms indicated that inclusion of the nonspecific storage effects can significantly improve the existing monoterpenoid emission models. Importantly, current emission models do not allow simulation of night emissions from the foliage of Mediterranean *Quercus* species [e.g., *Niinemets et al.*, 2002a] that can successfully be described by the dynamic model (Figure 8). Although the steady-state emission model employing the correlation between monoterpene emission and photosynthetic electron transport rate (ETR-model [*Niinemets et al.*, 2002c]) gave

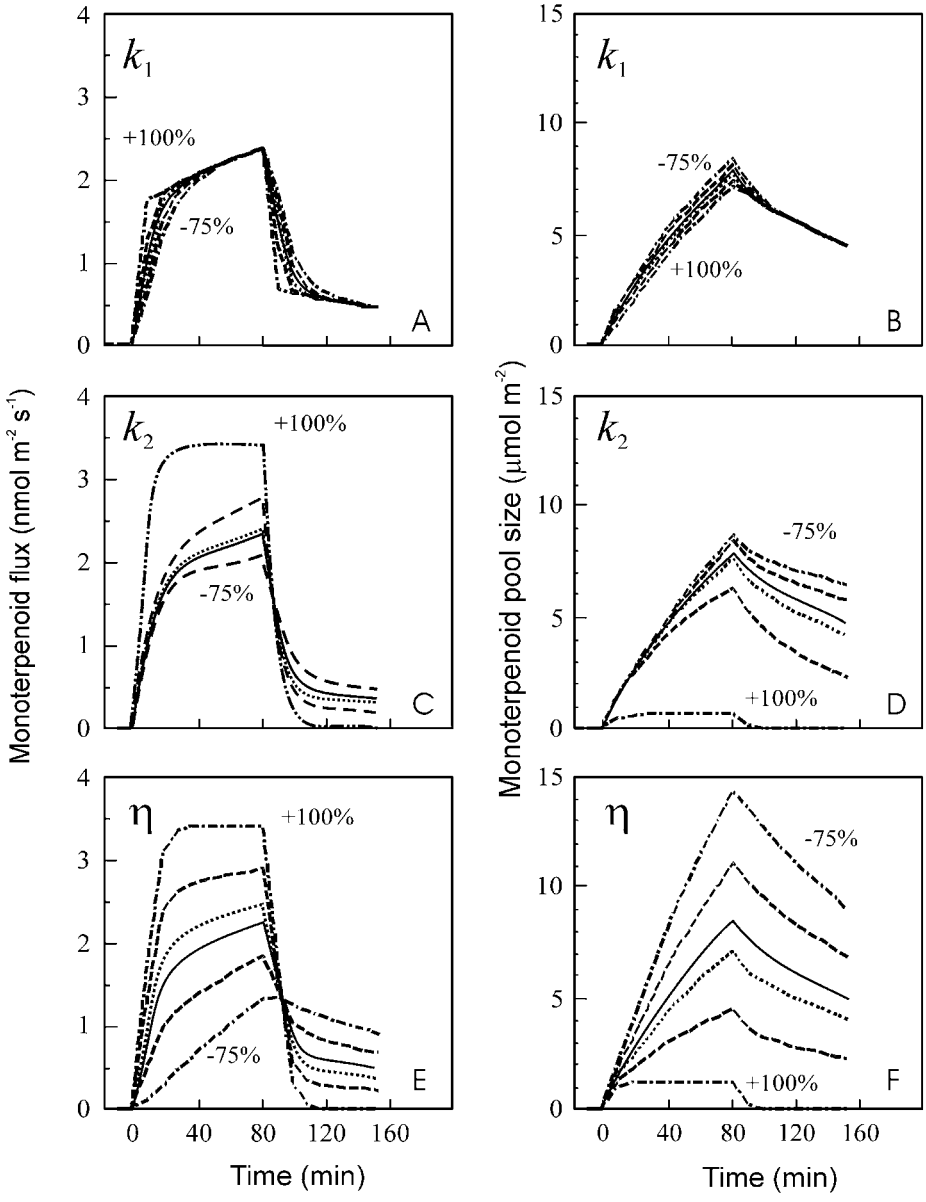

Figure 4. Sensitivity of the dynamics of monoterpene emission rate to changes in the decay constants k_1 ("fast" storage pool, **A**) and k_2 ("slow" storage pool, **C**), and to changes in the fraction (η) of synthesized monoterpenoids going into the "fast" storage pool (**E**, equations (1)–(3)); and corresponding modifications in the total monoterpenoid storage pool size (**B**, **D**, **F**). The default parameter values (solid line) of $k_1 = 2.46 \cdot 10^{-3}$ s^{-1}, $k_2 = 9.62 \cdot 10^{-5}$ s^{-1} (actual values for the total emission rate, Table 3) and $\eta = 0.5$ were changed by -75, -50, 25, 50 and 100% as indicated in the figure.

the same daily integrated monoterpene flux as the model version with nonspecific storage pools, the steady-state model overestimated peak fluxes compared to the dynamic model and Guenther et al. algorithm [*Guenther et al.*, 1993] that uses fixed temperature and light functions to describe the effect of environmental variables on monoterpenoid emission. However, because of missing nighttime emission rates, the Guenther et al. model underestimated the total daily emission rates. Thus, these simulation results further underscore the importance of the dynamic description of monoterpenoid emission rates in Mediterranean *Quercus* species.

3.5. Linking the Storage Characteristics to Monoterpenoid Physico-Chemical Variables

[42] The half-time of the "fast" pool (τ_1) was negatively correlated with the Henry's law constant (H, Figure 9a), but τ_1 was independent of monoterpenoid octanol to water partition coefficient ($K_{o/w}$, Figure 9b). Given that a negative relationship between H and storage pool half-time is

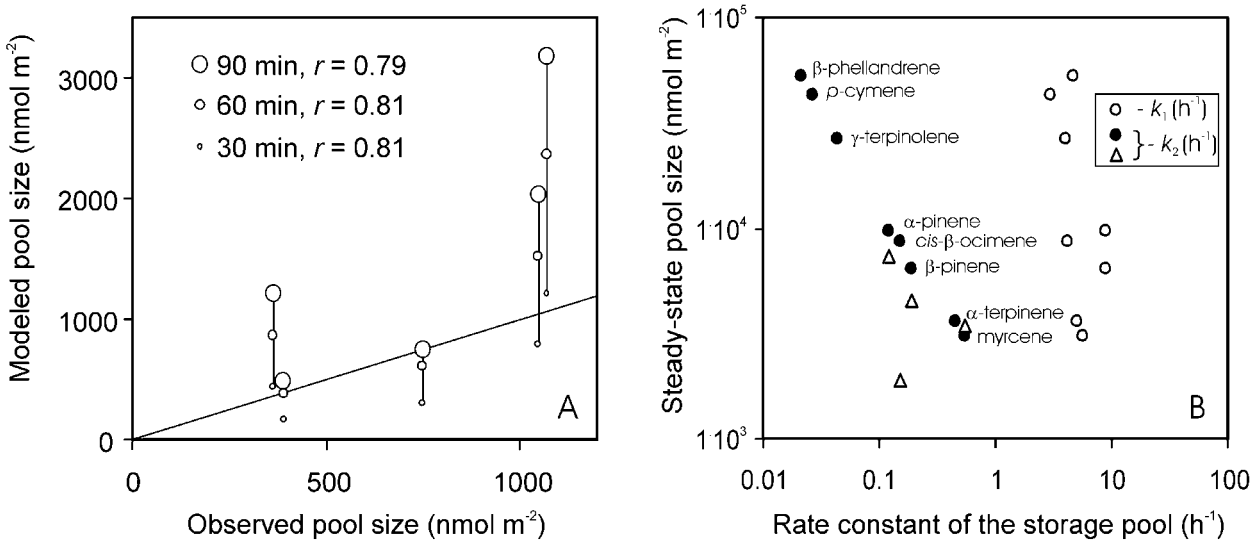

Figure 5. Modeled versus measured pool sizes (**A**) of various monoterpenoids of *Q. ilex*, and calculated steady-state pool size (**B**, equation (4)) versus the rate constant of the "fast" (open circles), and "slow" (filled circles and open triangles) storage pool. In **A**, the pool sizes are simulated for 30, 60, and 90 min periods of leaf exposure to continuous irradiance of 1000 μmol m^{-2} s^{-1} (equations (1)–(3), Table 3), whereas the leaf monoterpene contents were measured after 60 min of light exposure [*Loreto et al.*, 1998]. In **B**, the steady-state pool size was computed (filled and open circles) taking the rate of synthesis for each monoterpenoid equal to 2 nmol m^{-2} s^{-1}, and fixing the fraction of synthesized monoterpenoids going into the "fast" pool (η) at 0.85. In addition, the observed pool sizes in leaves of *Q. ilex* fumigated with high ambient air monoterpene concentrations (triangles, data of *Delfine et al.* [2000]) are also shown.

expected for monoterpenoid diffusion from leaf liquid phase (equation (12)), these relationships provide correlative evidence that the monoterpenoid "fast" pool is in the leaf liquid phase.

[43] The half-time of the "slow" pool (τ_2) was independent of H (Figure 9c), and was positively related to $K_{o/w}$ (Figure 9d), suggesting that the "slow" pool stems from leaf lipid phase (equation (15) and equation (22)). Association of the "slow" pool with leaf hydrophobic regions is further supported by a negative correlation between $K_{o/w}$ and the fraction of monoterpenoid going into the "fast" (aqueous) pool (η, Figure 9f).

3.6. Empirical Versus Theoretical Mesophyll Transfer Conductances

[44] The observed correlations (Figure 9) suggest a biophysical control on monoterpenoid emissions, with Henry's constant and $K_{o/w}$ as the most important parameters. Using the information of the likely location of nonspecific storage pools and using the classic diffusion theory, allows to link the rate constant k_1 to the mesophyll transfer conductance from the site of monoterpene synthesis and/or storage to the substomatal cavities (G_M, equation (12)), and the rate constant k_2 to the diffusion conductance from the lipid phase to substomatal cavities (equation (15)).

[45] The mesophyll diffusion conductance determined from k_1 was positively correlated with both the derived (equations (16)–(21)) liquid-phase (Figure 10a) and gas-phase (Figure 10b) conductance components of the total mesophyll diffusion conductance (Figure 10c). The estimates of G_M obtained from the time-constant of the "slow" pool were independent of the theoretical estimates ($r^2 = 0.04$, $P > 0.5$).

[46] Simulations indicated that the negative relationship between the half-time of the fast pool and Henry's law constant (Figure 9a) can be parameterized only when both the liquid- and gas-phase components of G_M are separately

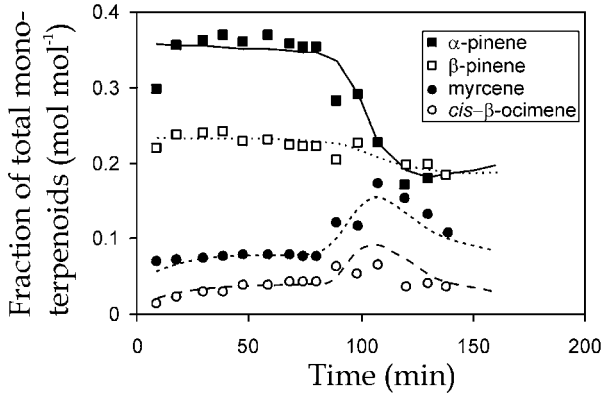

Figure 6. Measured [*Loreto et al.*, 1996a] and simulated (equations (1)–(3), Table 3) changes in the fractional composition of emitted monoterpenoids in *Q. ilex* during leaf illumination (0 min ≤ t ≤ 80 min) and darkening (t > 80 min). The same time-course as in Figure 3a.

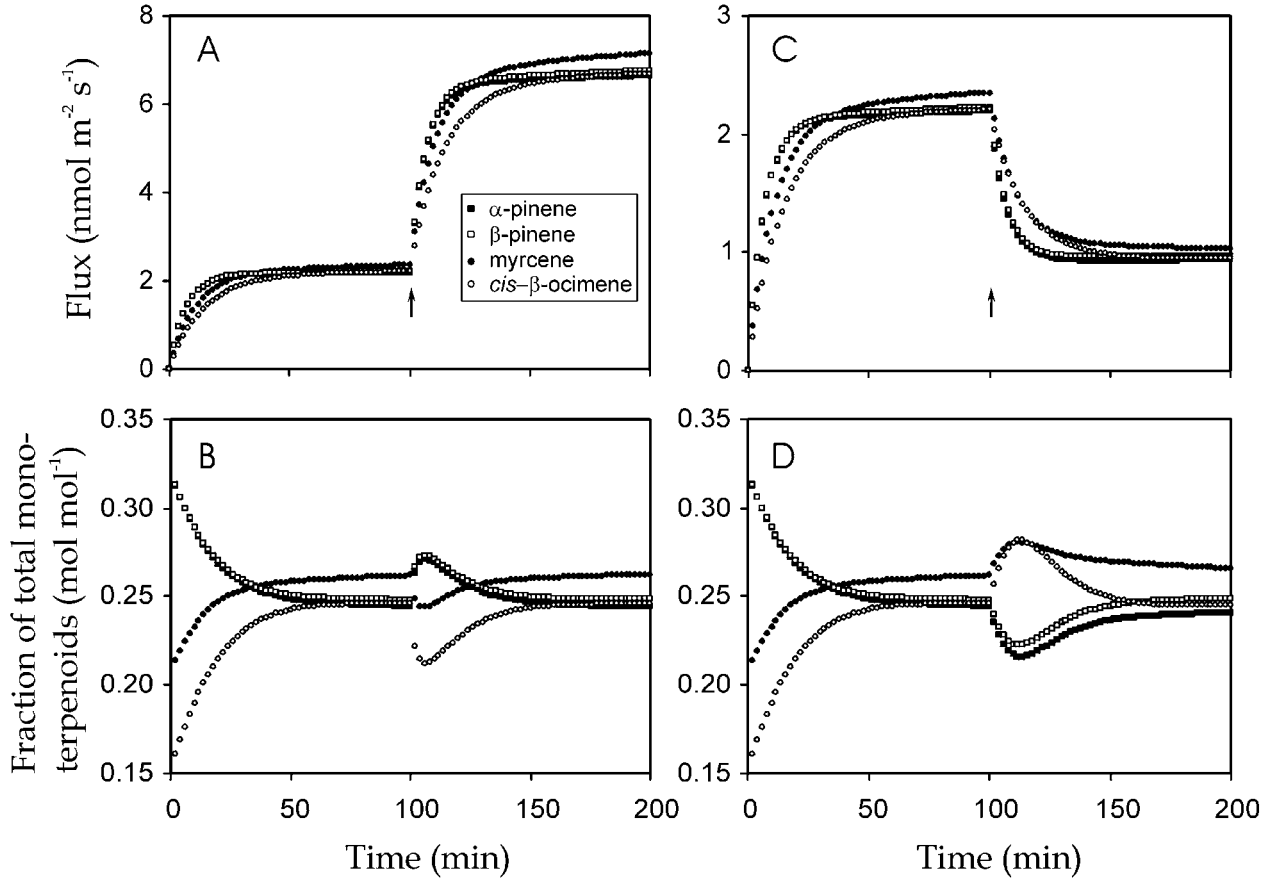

Figure 7. Simulated (equations (1)–(2b), Table 3) changes in monoterpenoid emission rate (**A**, **C**) and fractional composition (**B**, **D**) in response to rapid changes in monoterpenoid synthesis rate (I). At time t = 0, I was changed from 0 to 2.5 nmol m^{-2} s^{-1}, and at t = 100 min (shown by the arrow), I was either increased to 7.5 nmol m^{-2} s^{-1} (**A**, **B**) or decreased to 1 nmol m^{-2} s^{-1} (**C**, **D**) for all monoterpenoids. The initial storage pool sizes were zero at t = 0. In the steady-state, all monoterpenoids are emitted with a rate of 0.25 times the total rate.

fitted (Figure 11) further suggesting that the emission from the fast pool is affected by the diffusion in both the liquid and gas phases. The model fits of τ_1 versus H relationship demonstrated that it is hyperbolic as expected according to equation (12) rather than linear (cf. Figures 9a and 11). However, the magnitude of G_M values derived from k_1 cannot be explained by the detailed diffusion model. The theoretical model predicted that the conductances should be 10^3–10^4-fold higher than estimated from the data. Thus, the internal resistances appear to be much larger than expected based on our one-dimensional diffusion model.

[47] We also observed a strong correlation between the theoretical and experimental estimates of the lipid-phase conductance (G_L) when the experimental estimate of G_L was derived from the time constant of the "slow" pool (Figure 12). The estimate of G_L determined from the time constant of the "fast" pool was not related to the theoretical G_L estimate (r^2 = 0.04, P > 0.5), again confirming the hypothesis that the "slow" pool is associated with the lipid phase.

[48] Similarly to the estimate of G_M derived from k_1, G_L determined from k_2 was 10^2–10^3-fold lower than the conductance calculated using *Q. ilex* leaf structural and monoterpenoid physico-chemical characteristics (equation (22)).

4. Discussion

4.1. Phenomenological Description of the Emission From the Storage Pools

[49] Although Mediterranean monoterpene-emitting *Quercus* species do not possess specialized terpene-storage compartments in the leaves, direct measurements of leaf monoterpene contents [*Loreto et al.*, 1998, 2000; *Delfine et al.*, 2000] indicate that there is a nonspecific foliar monoterpenoid pool, emission from which may significantly alter the emission dynamics in these species. Thus, relevant time-lags may exist between the synthesis and emission of monoterpenoids also in species lacking monoterpenoid storage tissues in the leaves [*Loreto et al.*, 1996a; *Ciccioli et al.*, 1997].

[50] We constructed a phenomenological emission model (equations (1)–(3), Figure 2) to explore the extent to which nonspecific monoterpenoid storage may alter the relationship between monoterpene production in the chloroplasts and emission through the stomata. Based on the empirical evi-

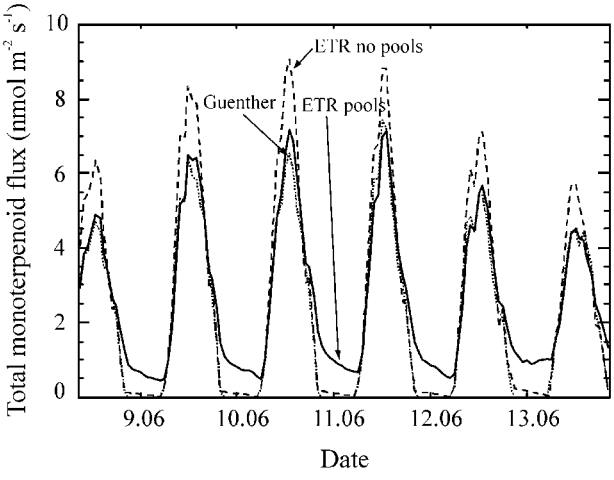

Figure 8. Modeled canopy monoterpenoid emissions at the Castelporziano test site in June 1997 (Reichstein et al., submitted manuscript, 2002) according to different leaf-level emission models. The Guenther et al. model [*Guenther et al.*, 1993] scales the emission rates to different leaf temperatures and incident quantum flux densities using an empirical algorithm, whereas the correlation between the rates of photosynthetic electron transport and monoterpene emission are employed in the ETR model [*Niinemets et al.*, 2002c]. In the original Guenther et al. and ETR-models, synthesized monoterpenoids are immediately emitted, whereas in the ETR model version with nonspecific storage pools, the monoterpenoids synthesized with a rate I, are emitted according to the dynamics described by equations (1)–(3) (Figure 2). The rate constants k_1 and k_2 were adjusted to the ambient temperature by a Q_{10} (the value of the rate constant at a temperature of $T + 10$°C to the rate at T) of 2.5 [*Niinemets et al.*, 2002a] (Reichstein et al., submitted manuscript, 2002).

dence that a single-exponential decay model provided poor, but double-exponential decay model excellent fits to the data (Figure 1), we divided the nonspecific monoterpene storage between two pools of differing decay constants. In addition to this experimental evidence, existence of at least two kinetically different monoterpenoid storage pools is also supported by ^{13}C-labeling and unlabeling studies in *Q. ilex* [*Loreto et al.*, 2000] and *Helianthus annuus* [*Heiden et al.*, 1999].

[51] Sensitivity analyses demonstrated (Figure 4) that the nonspecific monoterpenoid storage significantly alters the emission dynamics in Mediterranean *Quercus* species. In fact, our simulations suggest that in natural conditions with strongly fluctuating environmental factors, monoterpene emission rates are never in a steady state. Although the rates of isoprenoid synthesis may be regulated very rapidly after light or temperature changes [*Singsaas et al.*, 1999; *Logan et al.*, 2000], the responses of emission rates to alterations in environmental factors are inherently constrained because of the storage phenomena. According to the simulations, such effects may importantly alter not only leaf-level monoterpene fluxes, but also strongly modify the dynamics of whole-canopy monoterpenoid flux (Figure 8).

[52] An important consequence of the nonspecific storage is the existence of nighttime emission fluxes of monoterpenoids. Such emissions have been observed in cuvette measurements in the field [*Niinemets et al.*, 2002a]. Unfortunately, canopy scale flux measurements are generally conducted only at daytime [*Moncrieff et al.*, 1997; *Valentini et al.*, 1997; *Fuentes et al.*, 2000], because the night fluxes are assumed to be zero, but also because of other difficulties associated with nighttime measurements like advection [*Lee*, 1998; *Aubinet et al.*, 2000]. Nevertheless, there is evidence of high atmospheric monoterpene mixing ratios at night in broad-leaved deciduous forests [*Fuentes et al.*, 1996], and we plead that future canopy-scale flux measurements are conducted over the entire daily time-course. Alternatively, nighttime leaf-level cuvette measurements or model estimations may be scaled to the canopy level, and used as a substitute of canopy level flux measurements. Using modeled rather than measured fluxes to correct for nighttime advection and ecosystem storage effects is a general praxis in large-scale carbon flux measurements [*Aubinet et al.*, 2000].

[53] It is tempting to use simple monoterpenoid emission algorithms that are driven only by incident light and leaf temperature and that assume that the rates of monoterpenoid production and emission are equal [*Bertin et al.*, 1997; *Ciccioli et al.*, 1997; *Niinemets et al.*, 2002c]. Because most of the nonspecific monoterpene storage is in the "fast" pool, these models may easily be parameterized to successfully simulate daily mean monoterpenoid emission flux. Furthermore, there are multiple problems associated with reliable large-scale monoterpene flux measurements [*Fuentes et al.*, 2000], and it may be disputed whether inclusion of further details can significantly improve the correspondence between measured and modeled canopy-level flux data. However, it is important to recognize that all steady-state algorithms will produce biased estimates after any change in environmental factors. Although the time-resolution of current eddy-accumulation flux measurements is relatively low, the half-times of the "slow" storage pools are on the order of hours. Thus, even for the available stand-level estimates, improved agreement between measured and simulated daily time-courses of monoterpene emission may be achieved by including the nonspecific storage effects into the emission algorithms (Figure 8).

[54] Previously, *Schuh et al.* [1997] have used the original Guenther et al. isoprene emission algorithm [*Guenther et al.*, 1993] to simulate the monoterpenoid emission during the daytime, and coupled the emission to temperature only at nighttime to describe the efflux from nonspecific storage pools in *Fagus sylvatica* and *Helianthus annuus*. However, it is important to recognize that whenever there is some monoterpenoid accumulation in the leaves, it may effectively untie the emission from synthesis also in illuminated leaves (Figures 4, 7, and 8).

4.2. What is the Capacity of Foliar Nonspecific Storage Pools?

[55] The leaves of *Q. ilex* have significant monoterpene contents even after 11 h of darkness [*Loreto et al.*, 2000].

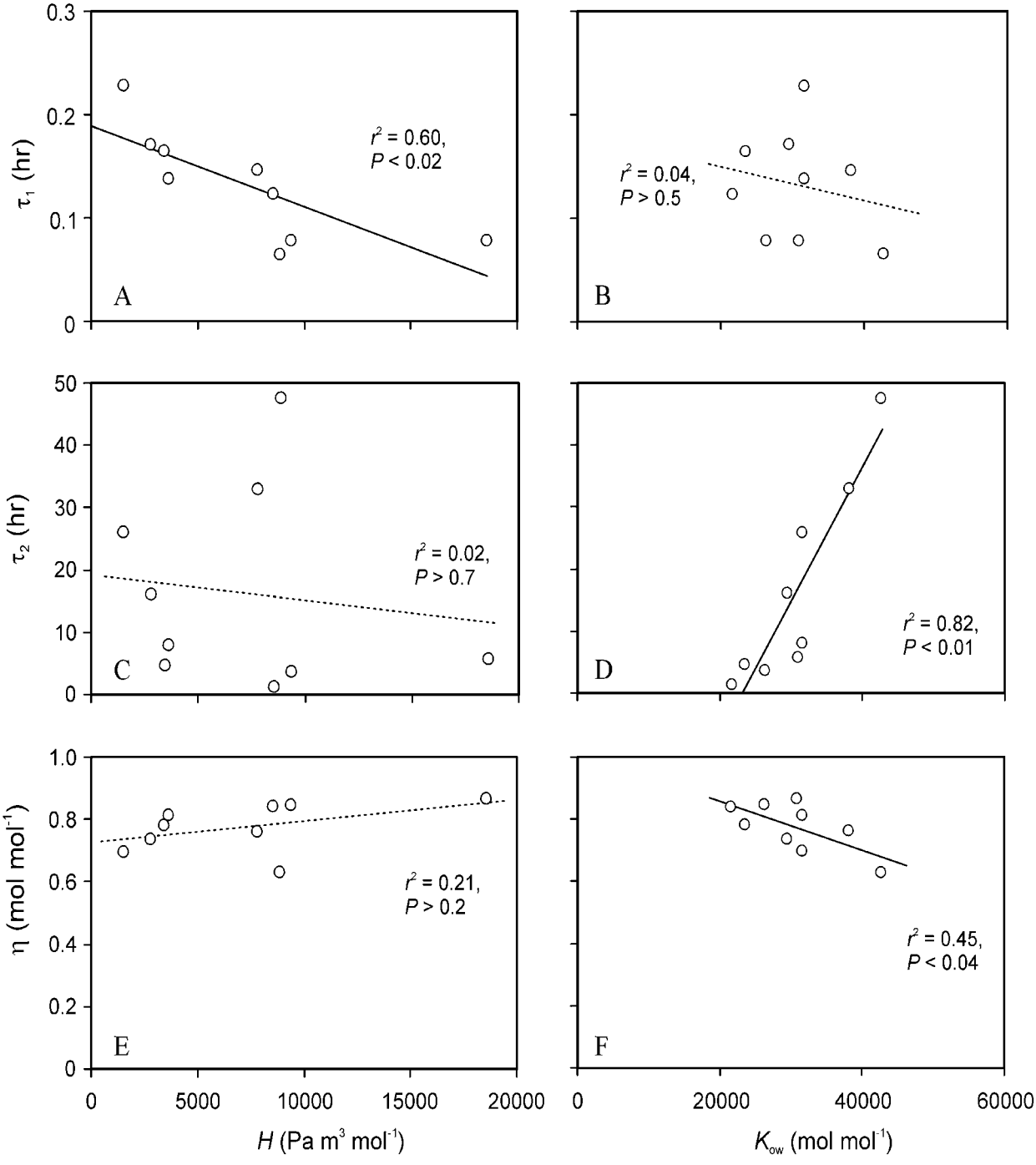

Figure 9. Correlation of the half-times of the "fast" (τ_1, **A**, **B**) and the "slow" (τ_2, **C**, **D**) monoterpenoid storage pools and the fraction of terpenes going into "fast" pool (η, **E**, **F**) with the monoterpenoid Henry's law constant (**A**, **C**, **E**), and octanol–water partitioning coefficient (**B**, **D**, **F**). The parameters of the dynamic monoterpene emission model (equations (1)–(4), Table 3) for *Q. ilex* were derived from *Loreto et al.* [1996a]. The data are fitted by linear regressions. Nonsignificant relationships are shown by punctuated lines. H was calculated for 30°C as described in Appendix A.

Similarly, monoterpene-fumigated leaves of nonemitting species *Q. suber* contain detectable amounts of monoterpenes 12 h after fumigation [*Delfine et al.*, 2000]. Long-term experiments further indicate that ^{13}C-labeled monoterpenoids are emitted from the leaves of *Helianthus annuus* more than 500 h after labeling [*Heiden et al.*, 1999]. Thus, monoterpenoid storage effects may even affect day-to-day emission dynamics, especially when the

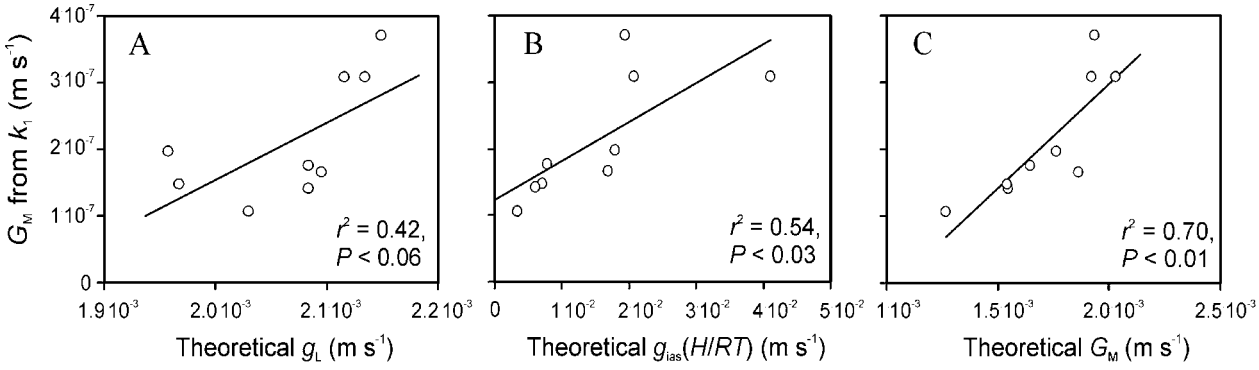

Figure 10. Comparison of the monoterpenoid mesophyll transfer conductances from the site of storage to substomatal cavities (G_M) derived from the rate constant of the "fast" monoterpenoid storage pool (k_1, equation (12), Table 3) with the mesophyll transfer conductances determined from leaf structural characteristics (equations (16)–(17), Table 2). The experimental conductance estimates are given in relation to (**A**) liquid-phase conductance from chloroplasts to outer surface of cell walls (g_L), (**B**) gas-phase conductance from outer surface of cell walls to substomatal cavities, and (**C**) the total mesophyll conductance from chloroplasts to substomatal cavities (G_M, equation (9)). Because G_M is a liquid-phase conductance, the gas-phase conductance in **B** was converted to a liquid-phase equivalent conductance, $g_{ias}H/(RT)$, where H is the Henry's law constant, R is the gas constant, and T is the absolute temperature. The relationships were fitted by linear regressions.

environmental conditions differ between the days. We have previously provided evidence that on warm days that follow cool days, monoterpenoid emission from the leaves of *Q. ilex* is larger than predicted assuming a constant emission versus temperature response function for all days [*Niinemets et al.*, 2002a, 2002c]. This discrepancy from model prediction was assumed to arise from monoterpenoid accumulation in cold days and emission in subsequent warmer days. Parameterization and assessment of the significance of such long-term storage influences requires knowledge of potential monoterpenoid pool sizes.

[56] The steady-state pool sizes calculated by our model (Figure 5b) are large enough to explain long-term storage effects on monoterpenoid emission kinetics. However, are these pool sizes realistic? Our simulations suggested that monoterpenoid pool sizes measured in leaves after a certain period of continuous light (Figure 5a) [*Loreto et al.*, 1998, 2000] are far from being in a steady state (Figure 5b). Nevertheless, monoterpene-fumigation experiments resulted in leaf monoterpene contents that closely approached the steady-state pool sizes calculated by our model in both monoterpene nonemitting species *Q. suber* and emitting species *Q. ilex* (Figure 5b) [*Delfine et al.*, 2000]. In light of these large pool sizes, we conclude that monoterpenoid storage may significantly alter long-term monoterpenoid emission dynamics. Existence of a long-term storage suggests that part of the variation in monoterpene emission rates in standardized conditions ("basal monoterpene emission factor") observed in recent studies in response to day-to-day fluctuations in leaf temperature [*Staudt and Bertin*, 1998; *Staudt et al.*, 2000] may partly result from the monoterpenoid storage effects.

[57] Our study along with the results of *Delfine et al.* [2000] further implies that nonspecific monoterpenoid storage effects may also occur in nonemitting species growing intermixed with the emitting species. Monoterpene uptake from ambient air, and emission in trace quantities may partly explain the contrasting literature observations of the potentials of certain species for monoterpene "production" [*Benjamin et al.*, 1997; *Owen et al.*, 1997]. Furthermore, the possibility that nonemitting species may form a terpene sink in situations with high air monoterpene mixing ratios, and be a source when the atmospheric monoterpene concentrations are low, suggests that the nonspecific storage effects may more importantly alter ecosystem monoterpene fluxes than they alter leaf level fluxes.

4.3. Changes in Emission Compositions Due to Storage Effects

[58] According to ^{13}C-labeling experiments, monoterpenoid labeling time-course may differ between various monoterpenoids [*Loreto et al.*, 1996a]. *Loreto et al.* [1996a] suggested that such differences in labeling may be indicative of interconversion between various monoterpenoids, differing regulation of synthesis rates, or of variation in monoterpenoid gas- to liquid-phase partitioning characteristics. Our simulations indicated that the monoterpenoid differences in storage characteristics (Table 3) may largely explain the differences in emission kinetics (Figures 7a and 7c). Furthermore, different time-courses of emission also bring along important temporal modifications in the fractional composition of emitted monoterpenoids (Figures 6, 7b, and 7d). Changes in the composition of emitted monoterpenoids have frequently been observed during the day, especially in species with extensive monoterpene storage pools [*Adams and Hagerman*, 1977; *Staudt et al.*, 1997, 2000; *Geron et al.*, 2000]. In these species, the fractional composition of emitted monoterpenes can be

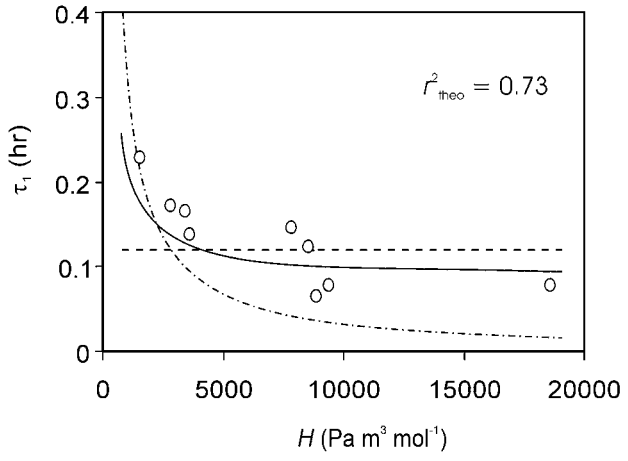

Figure 11. Relationship between the half-time of the "fast" pool and the monoterpenoid Henry's law constant. The solid line indicates the best fit to the data according to equation (12) ($g_L = 2.82 \cdot 10^{-7}$ m s^{-1}, $g_{ias} = 4.32 \cdot 10^{-7}$ m s^{-1}). Also shown are hypothetical relationships with either g_{ias} or g_L set at an average value determined from leaf anatomical characteristics (equations (16)–(17)), while fitting the other component of total mesophyll transfer conductance from chloroplasts to substomatal cavities (equation (9)) to the data by least squares regression. The dashed line demonstrates the best-fit relationship for g_{ias} set at $5.4 \cdot 10^{-3}$ m s^{-1} and g_L fitted ($g_L = 2.01 \cdot 10^{-7}$ m s^{-1}). The dot-dashed curve gives the relationship for g_L set at $2.1 \cdot 10^{-3}$ m s^{-1} and g_{ias} fitted ($g_{ias} = 1.86 \cdot 10^{-7}$ m s^{-1}). r^2_{theo} is the explained variance achieved with the best hyperbolic model.

different from the composition of immediately synthesized and stored monoterpenoids, but the explanations for such modifications have been lacking so far.

[59] Apart from light and temperature, which are the primary drivers controlling monoterpene synthesis, decreases in air humidity may also moderately decrease monoterpene emission rate [*Guenther et al.*, 1991; *Loreto et al.*, 1996a, 1996c], but it is not clear how. The humidity may even more strongly control the composition of the emitted monoterpenoids than the emission rates. For example, *Loreto et al.* [1996a] observed in *Q. ilex* an increase in *cis*-β-ocimene emission relative to α-pinene emission after a decrease in cuvette air humidity. According to our simulations (Figures 7c and 7d) such an effect would be expected after a moderate decline in monoterpene synthesis rate. Of course, selective regulation of specific monoterpene synthases triggered by changes in stomatal conductance [*Niinemets et al.*, 2002b] may further modify the monoterpene compositions.

[60] Various monoterpenoids largely differ with respect to the gas-phase rate coefficients for reaction with ozone and hydroxyl radicals [*Fehsenfeld et al.*, 1992; *Guenther et al.*, 1994], e.g., both these rate constants are an order of magnitude larger for cis-β-ocimene than for α-pinene [*Calogirou et al.*, 1996; *Howard and Meylan*, 1997]. Thus, simulations of atmospheric reactivity require not only accurate description of total monoterpenoid fluxes, but also the fractional compositions of emitted monoterpenoids (Figure 7). Because of the importance of reliable description of monoterpenoid composition, species-specific emission patterns along with species abundance estimates have been employed to describe large-scale variabilities in the emission composition [*Geron et al.*, 2000]. We suggest that dynamic monoterpenoid emission models have a large potential to further improve the predictions of emission compositions.

4.4. Correlations Between the Pool Time Constants and Monoterpenoid Physico-Chemical Characteristics

[61] Plant volatile isoprenoids form a chemically divergent group of compounds including aliphatic and cyclic hydrocarbons, alcohols, aldehydes, and ketones that have widely differing physico-chemical characteristics such as diffusion coefficients in air and water, solubilities in water and lipids, as well as saturated vapor pressures (Table 1). Moreover, there is also a significant variation among structurally similar compounds such as monoterpene hydrocarbons. This is important, because the key physico-chemical characteristics may strongly affect the monoterpenoid diffusion flux from the site of synthesis to the ambient air in non-steady-state conditions. *Tingey et al.* [1991] have previously developed a monoterpene emission model based on monoterpenoid physico-chemical variables. However, application of such models is currently seriously hampered by the lack of relevant monoterpene physico-chemical variables.

[62] The mechanistic flow/conductance model (equations (5)–(15)) indicated that monoterpenoid diffusion coefficients in air-, water, and lipids, and equilibrium air to water

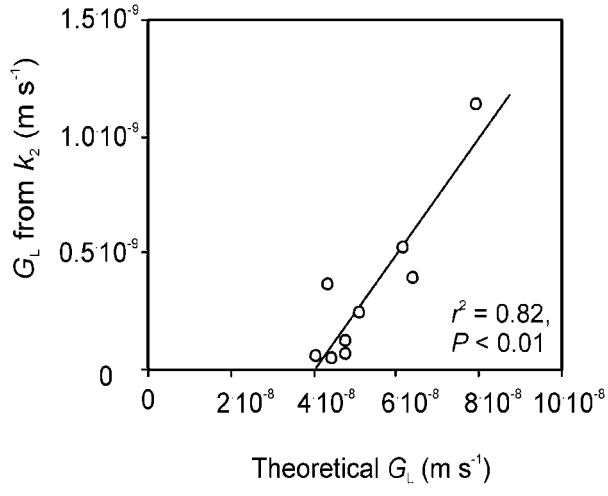

Figure 12. Correlation between the leaf lipid-phase conductance determined from the kinetics of the "slow" monoterpenoid storage pool (equation (15), Table 3), and the conductance (equation (22)) calculated using the structural characteristics of *Q. ilex* leaves (Table 2) and monoterpenoid lipid-phase diffusion coefficients determined from chloroplast membrane permeability.

(Henry's law constant) and lipid to water partition coefficients are the primary physico-chemical variables required to associate the kinetic constants of our phenomenological model to leaf structure and monoterpenoid characteristics. We determined the diffusion coefficients using quantitative structure/property relationships (equation (23), Appendix A). For the partition coefficients, we gave preference to experimentally determined values, because of large errors associated with prediction of these characteristics from correlative relationships [*Grain*, 1990b; *Fichan et al.*, 1999], and because these methods do not allow to distinguish between structurally related compounds.

[63] For specific monoterpenoids (Appendix A), there were also large study-to-study variabilities in the experimental estimates of solubility and vapor pressure that were required to calculate Henry's law constant (H, equation (8)). Given that the experimental estimation of low-temperature monoterpenoid vapor pressures ranging from 3 to 600 Pa at 25°C (Table 1) is inherently imprecise, we critically reviewed a large amount of data sources and calculated vapor pressures for specific temperatures using the Antoine equations (equation (A5)) derived from the data (Appendix A). Although monoterpenoid aqueous solubility estimates were also determined from an extensive set of data sources, determination of solubility limits of sparingly soluble organics is particularly complicated, because of adsorption of chemicals onto glassware, and formation of colloidal aggregates in the saturated solutions [*McAuliffe*, 1969; *Mackay and Shiu*, 1981; *Staudinger and Roberts*, 1996]. Thus, the vapor pressures revised in the current study are likely more reliable than the aqueous solubilities (Table 1, Appendix A). Nevertheless, we suggest that the critical revision of both vapor pressures and aqueous solubilities allowed us to obtain best achievable estimates of Henry's law constant (Table 1).

[64] We observed a negative correlation between the half-time of the "fast" pool and H (Figure 9a), and a positive correlation between the half-time of the "slow" pool and octanol to water partition coefficient ($K_{o/w}$, Figure 9d). Given also that the fraction of monoterpenoids going into the "fast" pool was negatively related to $K_{o/w}$ (Figure 9f) we suggested that the "fast" pool is in the aqueous phase, and the "slow" pool is in the leaf lipid phase. Linking the kinetic constants of the phenomenological emission model to the conductances of the mechanistic flow/conductance diffusion model (equations (12) and (15)) yielded also good correlations between the theoretical and empirical conductance estimates (Figures 10–12) further supporting our hypotheses of the location of the pools.

[65] Although there were significant discrepancies between the magnitude of the empirical and theoretical conductance estimates (Figures 10–12), the obtained correlations (Figures 9a and 9d) may still be employed to gain insight into the possible range of variation of the pool half-times and make inferences of the significance of nonspecific storage phenomena for various monoterpenoids, physico-chemical characteristics of which widely vary (Table 1). For the nine monoterpenoids used for model parameterization (Table 3), the range of the half-times of the "fast" pool (τ_1) varied from 0.0652 to 0.228 h, whereas that of the "slow" pool (τ_2) varied from 1.26 to 47.6 h. For the 22 monoterpenoids emitted by *Q. ilex*, the hyperbolic relationship of τ_1 versus H in Figure 11, and linear regression of τ_2 versus $K_{o/w}$ in Figure 9d, provided a range of 0.07–10.4 h for τ_1, and 0.66–42.3 h for τ_2, further indicating that monoterpenoid physico-chemical characteristics significantly alter the emission kinetics of various plant volatiles.

[66] The range of τ_1 obtained by regression analysis is beyond our measurements, and should be interpreted with caution. These high values of τ_1 were predicted for compounds with relatively low H—camphor, 1,8-cineole, linalool and α-terpineol (Table 1). Nevertheless, high liquid-pool half-times in these compounds are also corroborated by experimental studies [*Loreto et al.*, 1996a; *Niinemets et al.*, 2002b] as well as by model simulations [*Niinemets et al.*, 2002b]. In fact, these compounds also have low $K_{o/w}$, suggesting that nonspecific storage pool essentially resides in the liquid-pool, and that the diffusion flux from the lipid phase insignificantly contributes to the emission.

[67] We only investigated the monoterpenoids emitted by *Q. ilex*, but this species also emits a sesquiterpene—caryophyllene—in low quantities, especially at higher temperatures [*Staudt and Bertin*, 1998]. Sesquiterpenes are emitted by many other plant species as well [*Ciccioli et al.*, 1999; *Hansen and Seufert*, 1999; *Heiden et al.*, 1999]. Given that sesquiterpenes have considerably lower vapor pressures and are more hydrophobic than monoterpenes [*Ciccioli et al.*, 1999], we expect for sesquiterpenes even larger half-times for the liquid and lipid pools.

4.5. Terpene Efflux Rates Continue Longer than Predicted by the Theoretical Diffusion Model

[68] Although the theoretical calculations of mesophyll diffusion conductance (equations (5)–(22)) have been demonstrated to provide realistic estimates of CO_2 diffusion conductance in *Q. ilex* [*Niinemets et al.*, 2002b], they significantly overestimated the actual time constants of the volatile pools (Figures 10–12). Possible sources for this overestimation may be: (1) contribution of newly synthesized monoterpenoids to emission fluxes that were assumed to originate from the storage only, e.g., after leaf darkening; (2) inaccuracies associated with physico-chemical characteristics of monoterpenoids; (3) errors in the estimates of theoretical diffusion conductances; (4) missing consideration of certain physico-chemical processes that affect diffusion, e.g. monoterpenoid adsorption/desorption.

[69] The derivations of the time constants of nonspecific storage pools assumed that monoterpenoid synthesis completely stops in the darkness. Yet, it cannot currently entirely be ruled out that some monoterpenoid synthesis continues after leaf darkening [*Loreto et al.*, 2000; *Shao et al.*, 2001]. *De novo* monoterpene synthesis increases the apparent half-times of the storage pools, and may partly explain the discrepancies between observations and theoretical calculations. Nevertheless, there is currently no conclusive evidence that the monoterpenoid synthesis does continue in the dark. Both ^{13}C labeling experiments [*Heiden et al.*, 1999; *Loreto et al.*, 2000] and the emission kinetics in the monoterpene-fumigated leaves of *Q. suber*—a species that

lacks monoterpene synthesis [*Delfine et al.*, 2000]—all indicate that terpene efflux may continue longer than 10 h at the expense of existing monoterpene pools. Furthermore, there should be no correlations between the pool-half times and monoterpenoid physico-chemical characteristics (Figure 9) when the major fraction of emitted monoterpenoids comes from *de novo* synthesis. Thus, we consider the possible *de novo* synthesis as an unlikely explanation for these discrepancies.

[70] Although we believe that we have obtained the best achievable set of physico-chemical variables of monoterpenoids, some discrepancies certainly arise from errors in these characteristics. Apart from the uncertainties discussed above, literature estimates of water solubility (δ) and octanol/water partition coefficient ($K_{o/w}$) were available for 25°C, but the laboratory emission measurements were conducted at 30°C. We scaled the Henry's law constant to various temperatures as the ratio of vapor pressure (equations (A5) and (A6)) to δ, and assuming that δ is independent of temperature for each monoterpenoid (Table 1). This routine predicted that H increased by 1.1- to 1.8-fold (on average 1.41) with a 5°C increase in leaf temperature for different monoterpenoids. This is consistent with experimental data demonstrating a strong effect of temperature on H [*Staudinger and Roberts*, 1996; *Rice et al.*, 1997]. For $K_{o/w}$, the temperature dependencies were not available, and the values measured at 25°C were employed. Although for hydrophobic compounds, $K_{o/w}$ may decrease with increasing temperature [*Lei et al.*, 2000], the enthalpy of octanol to water transfer is generally relatively low, implying minor temperature effects on $K_{o/w}$ [*Sangster*, 1989]. We conclude that more experimental work on temperature effects on monoterpene solubility in water and plant lipids is necessary, but also that the uncertainties in the H and $K_{o/w}$ values led to errors less than an order of magnitude. Given this and also that these errors were unlikely systematic, they cannot be the sole reason for large systematic differences between the conductance estimates.

[71] As we discussed, the possible overestimation of monoterpenoid diffusion conductances due to the use of the same gas-phase tortuosity and cell wall effective porosity as determined for CO_2 diffusion in the leaf likely leads to errors less than an order of magnitude. However, more importantly, our theoretical calculations explicitly suggested that stored foliar monoterpenoids are homogeneously distributed within the leaf cells. This does not consider that highly lipophilic monoterpene molecules may aggregate in the cytosol creating micelles and vesicles. Such an aggregation of monoterpenes into micelles and droplets of pure monoterpenoids may dramatically decrease the effective surface area for diffusion. Because plant cells generally contain lipid vesicles, and monoterpenoid aggregation may easily decrease the diffusion surface area by a factor of 10^3–10^4 (Figure 10) we consider this possibility as a most likely explanation for the discrepancies between observations and simulations of the "fast" pool time kinetics.

[72] Our theoretical calculations further assumed that the diffusion proceeds along the shortest pathway from the chloroplasts to substomatal cavities, and that the length of the diffusion pathway is a constant. This may be appropriate if the diffusion efflux rates are high due to high rates of synthesis. However, all chloroplast membranes will gradually come to an equilibrium with the aqueous phase, and after cessation of the synthesis, a large fraction of monoterpenes may diffuse from the distal sides of the chloroplasts and cytosol, indicating that a series of exponentials may be appropriate to describe the time-dependent changes in monoterpenoid emission in such a situation. This is a general limitation of flow/resistance diffusion models [*Parkhurst*, 1994]. In addition, leaves also contain significant amounts of vasculature and epidermal tissues that may also form a sink of monoterpenoids during high rates of synthesis, but present a source after cessation of synthesis. To account for the inherent heterogeneities of the diffusion pathway, we suggest that explicit three-dimensional models may provide an important tool to improve the description of monoterpenoid diffusion within the leaves.

[73] The lumped leaf lipid phase is actually any hydrophobic location in the leaf including cuticle, cell wall lignin, and all leaf membranes, being thus, inherently heterogeneous. Because of missing measurements of water to lipid-phase partition coefficients, $K_{o/w}$ was used as an estimate of monoterpenoid solubility in the leaf lipid fraction (equations (14) and (22)). This was partly verified by the circumstance that the monoterpenoid $K_{o/w}$ and cuticle to water partition coefficient were essentially equal. However, further work is called for to determine the monoterpene solubilities of various leaf hydrophobic regions. Given that the estimates of monoterpenoid diffusivity in different leaf membranes and cuticle varied by three orders of magnitude (10^{-14}–10^{-16}, equations (22)–(23)), the calculations of the "slow" pool half-times may be improved by actual measurements of monoterpenoid diffusivities in various components of leaf lipid phase.

[74] Our calculations of the diffusion conductances were based on the assumption that there is no interaction between the diffusing compound and the diffusion medium. However, adsorption to the surface, e.g., to hydrophobic surfaces of leaf apoplast, may strongly curb the effective diffusion conductances. The more hydrophobic a chemical, the more susceptible is it to adsorption due to increases in van der Waals and hydrophobic forces [*Staudinger and Roberts*, 1996]. Studies indicate that monoterpenoids are especially vulnerable to adsorption [*Jørgensen et al.*, 1999]. This is important because the adsorption effects can significantly decrease the effective compound diffusion coefficient, depending on the relative magnitude of pore volume diffusion and diffusion in the adsorbed phase, i.e., surface diffusion [*Drazer et al.*, 1999; *Prasetyo et al.*, 2002; *Sotelo et al.*, 2002]. Surface diffusion is generally several orders of magnitude slower than the pore volume diffusion [*Drazer et al.*, 1999; *Prasetyo et al.*, 2002] suggesting that monoterpenoid adsorption to porous hydrophobic apoplast surface may provide a further explanation for the large half-times of the "slow" pool.

4.6. Outlook

[75] The outlined complications indicate that the theoretical estimations of monoterpenoid diffusion conductances

are currently bound to inherent uncertainties, and that further detailed experimental work is required to gain mechanistic insight into within-leaf diffusion of monoterpenoids. Although it may first seem that our approach requires an excessive number of parameters, being therefore, inferior to the existing empirical algorithms [*Guenther et al.*, 1993], most of these parameters are monoterpenoid physico-chemical characteristics, exact estimates of which are either available or may be determined in the laboratory. Once determined, these characteristics can always be taken as constants. In fact, our phenomenological model needs three parameters per monoterpenoid, of which two are needed to describe the kinetics of the liquid and lipid phases, and one is needed to distribute the synthesized monoterpenoids between the pools. For the time being, we suggest that empirical correlations between nonspecific storage pool half-times and physico-chemical characteristics of volatile monoterpenoids provide an encouraging way to determine these kinetic constants, and include the storage effects into current emission models. In the future model generalization, and after more species with contrasting emission patterns have been investigated, time-lags in the synthesis and emission that are important at ecosystem, regional and global scales may possibly be characterized by a single empirical delay factor.

5. Conclusions

[76] Our simulation analysis demonstrates that nonspecific storage effects importantly alter monoterpenoid emission dynamics to rapid and long-term changes in environmental conditions in emitting species that lack specialized monoterpene-storage compartments in the leaves. Current steady-state emission models generally provide poor fits to daily time-courses of monoterpenoid emission in these species, suggesting that the models still lack important mechanisms. For example, they do not account for the delays between monoterpene production and emission due to nonspecific storage. There are large diurnal and day-to-day variabilities in environmental factors, making consideration of such effects pertinent, especially for midday periods of high atmospheric reactivity, during which it is especially relevant to reliably predict the emission rates. In addition, nonemitting species may form a significant sink for monoterpenoids, in particular, when atmospheric monoterpene mixing ratios are high, suggesting that the nonspecific storage effects may become amplified at an ecosystem level.

[77] A further outcome of this study is that the nonspecific storage brings about modifications in the fractional composition of emitted monoterpenoids after changes in environmental conditions. Although such modifications in terpene composition are often observed, they cannot be explained by current empirical steady-state models. Given that for various plant monoterpenoids the atmospheric rate constants for reaction with ozone vary more than four orders of magnitude [*Calogirou et al.*, 1996] and for the reaction with hydroxyl radicals more than two orders of magnitude [*Howard and Meylan*, 1997], prediction of shifts in monoterpene fractional composition has major significance for constructing atmospheric reactivity scenarios.

[78] Encouraging correlations were observed between monoterpenoid physico-chemical characteristics and turnover times of nonspecific storage pools, providing an important basis to evaluate the potential storage effects for various monoterpenoids. However, discrepancies between the empirical and theoretical monoterpenoid conductances from the site of storage to substomatal cavities indicated that further research is necessary to determine the distribution of stored monoterpenoids within the leaves.

[79] Mediterranean *Quercus* species provide a good example of a system where the emission rates are controlled both by physiology and storage pool sizes. There is recent evidence indicating that monoterpene emission may originate from pools of differing time constant also in conifer species [*Schürmann et al.*, 1993; *Simon et al.*, 1994; *Staudt et al.*, 1997; *Shao et al.*, 2001], emission in which was previously thought to originate only from the resin ducts with a slow turnover time [e.g., *Tingey et al.*, 1991; *Guenther et al.*, 1993]. Assuming this, the terpene efflux rates have been related to leaf temperature only. We call into question the hypothesis that the emission fluxes in conifers are always in a steady state, and suggest that our analysis may potentially also be applied to monoterpene emitting species with extensive foliar storage tissues. To parameterize such effects, more advanced understanding of monoterpene partitioning between short-and long-term storage as well as of leaf internal diffusion pathway is necessary.

Appendix A: Physico-Chemical Characteristics of Isoprenoids

A1. Binary Diffusion Coefficients in Air

[80] The equation of Chapman and Enskog (cited by *Tucker and Nelken* [1982]) as modified by *Wilke and Lee* [1955] was employed to compute the binary diffusion coefficients of monoterpenoids in air (D_A, $m^2\ s^{-1}$) for a certain temperature (T_K, K) and air pressure (P, Pa). This method describes empirically the diffusion of gases by intermolecular collision:

$$D_A = \left(1.04 + 3.66\sqrt{1/M_{air} + 1/M_M}\right) \cdot 10^{-3} \frac{\sqrt{T_K^3}\sqrt{M_R}}{P\sigma^2\Omega}, \quad \text{(A1)}$$

where Ω is the collision integral, σ is the characteristic length of monoterpene molecule interacting with air molecules (Å) [*Wilke and Lee*, 1955], and M_R (mol g^{-1}) is given as $(M_{air} + M_M)/(M_{air}M_M)$, where M_{air} is the molar mass of air (29 g mol^{-1}) and M_M that of the monoterpenoid. The collision integral is a function of kT_k/ε, where k is the Boltzmann's constant ($1.38 \cdot 10^{-23}$ J K^{-1}), and ε the energy of attraction (J). Boiling points (K) of specific compounds are necessary to calculate Ω, and LeBas molar volumes (V'_M, $cm^3\ mol^{-1}$) to determine σ values [*Tucker and Nelken*, 1982]. LeBas molar volumes are calculated as a combination of atom- and structure-specific diffusion volume increments. This method is applicable over a large temperature and pressure range, and provides estimates of D_A with an average error of ca. 4% [*Tucker and Nelken*, 1982]. A comparison of calculated D_A values (equation (A1)) with experimental estimates of D_A [*Berezhnoi and*

Semenov, 1997] for alicyclic and aromatic hydrocarbons, aliphatics, and aliphatic alcohols—all major classes of compounds observed among volatile isoprenoids of *Q. ilex*—also indicated that equation (A1) gives estimates with a relative error of 0–9.4% (average 4.2% for $n = 11$).

[81] The binary diffusion coefficient for water vapor in air at normal pressure was calculated from an empirical equation summarizing a large amount of experimental data of various sources [*Vargaftik*, 1972], for a temperature range of 273 K < T_K < 370 K):

$$D_A = 2.232 \cdot 10^{-5} \left(\frac{T_K}{273.16} \right)^{1.81}, \quad \text{(A2)}$$

This equation provides a D_A value of $2.62 \cdot 10^{-5}$ m^2 s^{-1} at 25°C. For the same temperature, equation (A1) predicts a value of $2.60 \cdot 10^{-5}$ m^2 s^{-1}.

A2. Diffusion Coefficients in Water

[82] The method of *Hayduk and Laudie* [1974] as described by *Tucker and Nelken* [1982] was used to calculate the diffusion coefficients of isoprenoids in water (D_W, m^2 s^{-1}):

$$D_W = \frac{5.041 \cdot 10^{-12}}{\eta^{1.14} \left(V'_M \right)^{0.589}}, \quad \text{(A3)}$$

where η is the viscosity of water (Pa s), and V'_M the LeBas molar volume. For 87 solutes diffusing into water the equation (A4) predicted D_W values with an average error of 5.8% [*Hayduk and Laudie*, 1974].

[83] Experimental data [*Vargaftik*, 1972; *Weast et al.*, 1989; *Yeletskii*, 1991] over the temperature range of 273–440 K were combined and summarized by an empirical equation ($r^2 = 0.9994$)

$$\eta = 649.7 \frac{T_K{}^{-1.652}}{T_K - 238.7}. \quad \text{(A4)}$$

Equation (A4) is valid for diffusion in an infinitely dilute solution. In practice, equation (A4) provides good approximations to the experimental data if the concentration of solute is less than 50 mol m^{-3}. Because of very low solubility, this conditions was satisfied for all volatile isoprenoids emitted by Mediterranean *Quercus* species (Table 1).

A3. Isoprenoid Vapor Pressures

[84] Extensive search of relevant physical reference data collections as well as specific experimental studies [*Josephy and Radt*, 1948; *Jordan*, 1954; *Banerjee et al.*, 1980; *Lide and Kehiaian*, 1994; *Fugmann et al.*, 1997; *Howard and Meylan*, 1997; *Bauer et al.*, 1998; *Daubert et al.*, 1998; *Eggersdorfer*, 1998; *Fichan et al.*, 1999; *Fluka Chemie AG*, 1999; *Merck KGaA*, 1999] (see also R. L. Brown and S. E. Stein, Boiling point data, in NIST Chemistry WebBook, NIST Standard Reference Database Number 69, edited by P. J. Linstrom and W. G. Mallard, National Institute of Standards and Technology, Gaithersburg, Md., available at http://webbook.nist.gov, July, 2001) was carried out to find saturated monoterpene partial pressure (P_V) versus temperature relationships, data of P_V at various temperatures, and values of normal (P_V = 101.325 kPa) boiling points (T_B). The geometric isomers (*cis*, *trans*-) were considered separately, but the data for stereoisomers of specific monoterpenoids were pooled. Relying on most reliable data sources [e.g., *Daubert et al.*, 1998], the obtained data were critically revised. In general, all data converged well at high values of P_V—close to and at normal boiling point temperatures of 155–220°C—but large discrepancies were observed between various data at lower temperatures. Although P_V values at temperatures of 0–50°C are particularly important for environmental applications, the experimental determinations of P_V become increasingly inexact with decreasing temperature. Preference was given to most recent experimental [e.g., *Fichan et al.*, 1999] and revised [*Daubert et al.*, 1998] data, and a number of P_V values estimated by extrapolation beyond the range of measurements as well as older experimental observations [see, e.g., *Jordan*, 1954; *Howard and Meylan*, 1997] significantly biased according to novel information were declined.

[85] Equilibrium vapor pressure (kPa) versus temperature (T_K, K) relationships were fitted by Antoine equation that is often employed to describe pressure versus T_K dependencies over a limited range [*Grain*, 1990b]:

$$P_V = 10^{A - \frac{B}{T_K - C}}, \quad \text{(A5)}$$

where A (dimensionless), B (K) and C (K) are empirical coefficients. These coefficients were obtained by fitting LogP_V versus $A - B/(T_K - C)$ relationship by a nonlinear regression. Overall, equation (A5) provided good fits to the data with the fraction of explained variance (r^2) generally exceeding 0.999.

[86] For sabinene and *cis*- and *trans*-β-ocimene, which are emitted in large quantities in *Q. ilex* [*Staudt et al.*, 2001], experimental information of low temperature vapor pressures was not available. For these monoterpenoids, an estimate of P_V at 25°C ($P_V{}^{25}$) was derived from a correlation between T_B and values of $P_V{}^{25}$ available for other structurally similar monoterpenoids (r^2 = 0.89). The estimates of $P_V{}^{25}$ along with other available data were further employed in derivation of the Antoine relationships. For these two, and for other monoterpenoids with limited experimental observations, C in equation (A5) was computed according to Thompson's rule as $0.19T_B - 18$ [*Grain*, 1990b] before fitting the P_V versus T_K relationships.

[87] In their physico-chemical model of monoterpenoid emission, *Tingey et al.* [1991] extrapolated vapor pressure data of liquid camphor to temperatures, at which camphor is a solid. However, the vapor pressure of a solid is much lower than that of a hypothetical supercooled liquid, and it is important to include an appropriate correction for phase change. Most of the monoterpenoids emitted by *Q. ilex* (Table 1) [*Staudt et al.*, 2001] are liquids at an ambient temperature of 25°C. However, camphene (melting point, T_m = 50.2°C) and camphor (T_m = 178.5°C) are solids over the temperature range relevant for monoterpene emission from the foliage, and α-terpineol is a solid up to a temperature of 34.8°C [*Devon and Scott*, 1972; *Howard and*

Meylan, 1997; *Bauer et al.*, 1998; *Fluka Chemie AG*, 1999; *Merck KGaA*, 1999]. Thus, the Antoine equations of these compounds provide a low-temperature estimate of P_V for a hypothetical supercooled liquid. The vapor pressure for a solid (P_V^s) at temperature T (K) is obtained from the supercooled liquid vapor pressure (P_V^l) as [*Mackay and Shiu*, 1981; *Grain*, 1990b]:

$$P_V^s = P_V^l e^{\Delta S_f R^{-1}(1-T_m/T)}, \quad \text{(A6)}$$

where ΔS_f (J mol^{-1} K^{-1}) is the entropy of fusion, R is the gas constant (J mol^{-1} K^{-1}), and T_m is in K. The default value for ΔS_f is 56.6 J mol^{-1} K^{-1} [*Shiu and Mackay*, 1986; *Grain*, 1990b]. For camphene a literature value of 93.3 J mol^{-1} K^{-1} [*Daubert et al.*, 1998] was used. ΔS_f of 37.4 J mol^{-1} K^{-1} for camphor and 124 J mol^{-1} K^{-1} for α-terpineol were determined from the vapor pressure differences for supercooled liquid as calculated by equation (A5), and actual measurements of vapor pressures of solid compounds at 25°C [*Howard and Meylan*, 1997].

A4. Aqueous Solubilities and Henry's Law Constants

[88] Currently available prediction methods to derive estimates of water solubility (δ) using quantitative structure-property relationships [*Grain*, 1990a; *Lyman*, 1990; *Yalkowsky and Banerjee*, 1992; *Myrdal et al.*, 1995] are generally accurate only within an order of magnitude [*Lyman*, 1990]. UNIFAC (Uniquac functional group activity coefficients), the most widely accepted approach for solubility determination (see *Yalkowsky and Banerjee* [1992] for a review), predicts monoterpene solubilities with an average accuracy of only 220% [*Fichan et al.*, 1999] (C. Larroche, personal communication, 2000). Given this large uncertainty, we considered only experimentally determined monoterpene solubilities [*Massaldi and King*, 1973; *Banerjee et al.*, 1980; *Schmid et al.*, 1992; *Weidenhamer et al.*, 1993; *Loreto et al.*, 1996a; *Howard and Meylan*, 1997; *Fichan et al.*, 1999] in our model calculations.

[89] There are inherent limitations in experimental determinations of solubility limits of poorly soluble organics, which are mainly associated with solute adsorption effects as well as formation of colloidal particles [*McAuliffe*, 1969; *Mackay and Shiu*, 1981; *Dickhut et al.*, 1986; *Myrdal et al.*, 1995; *Staudinger and Roberts*, 1996], and lead to study-to-study variability among experimental estimations. Possibly because of experimental difficulties, we observed a large variability in δ for specific monoterpenoids. For example, for α-pinene the experimental determinations provided values ranging from 0.026 mol m^{-3} [*Schmid et al.*, 1992] to 0.16 mol m^{-3} [*Weidenhamer et al.*, 1993] at 25°C. Examination of the deviation of all available experimental data from the mean value indicated that certain studies provided biased solubility estimates; e.g., the study of *Weidenhamer et al.* [1993] gave consistently higher solubility estimates for monoterpenes with low solubility, and lower estimates for monoterpenes with higher solubility. Systematic deviation from other published data provided the criterion for declining the data. After declining the biased observations, a geometrical mean value was calculated for the monoterpenoids (Table 1).

[90] The Henry's law constants (H, Pa m^3 mol^{-1}) were calculated as the ratio of saturated vapor pressure, P_V, to aqueous solubility (equation (8)). The primary assumption of our H calculations is that the solubility of water in the pure organic compound is small (<0.05 mol fraction [*Staudinger and Roberts*, 1996]), i.e., that the vapor pressure of the water-saturated organic compound negligibly differs from the vapor pressure of the pure compound.

[91] The water solubility of organic compounds may increase, decrease or remain constant with increasing temperature. In general, the solubilities of most liquids and solids increase, and the solubilities of gases decrease with increasing temperature [*Yalkowsky and Banerjee*, 1992]. However, the data of temperature effects on monoterpenoid solubility are scarce. For limonene, a liquid monoterpene, the solubility increases over the temperature range of 0 to 25°C with an enthalpy of solution (ΔH_d) of 9.7 kJ mol^{-1} (calculated from *Massaldi and King* [1973]). However, for 1,8-cineole, δ measured at 20°C in one study [*Howard and Meylan*, 1997] was larger than that measured at 25°C [*Schmid et al.*, 1992; *Fichan et al.*, 1999]. For camphor, a solid monoterpene, experiments provide a δ value of 8.2 mol m^{-3} at 20°C [*Merck KGaA*, 1999], 10.5 mol m^{-3} at 25°C [*Howard and Meylan*, 1997], and 10.6 mol m^{-3} at 39°C [*Josephy and Radt*, 1948]. For another solid monoterpenoid, borneol, δ = 4.51 mol m^{-3} at 20°C, and δ = 4.84 mol m^{-3} at 25°C [*Josephy and Radt*, 1948]. Potentially large variability in experimental solubility determinations, especially if the data from various sources must be pooled, complicates the assessment of temperature effects on solubility, and evaluation of the accuracy of ΔH_d values obtained. Nevertheless, available data collectively demonstrate minor temperature effects on the solubility of liquid and solid monoterpenoids. Thus, we scaled the Henry's law constant to each temperature by determining P_V from equations (A5) and (A6), and assuming an invariable water solubility of specific monoterpenoid (Table 1).

A5. Octanol/Water Partition Coefficients

[92] Experimental determinations of monoterpenoid octanol to water partition coefficients ($K_{o/w}$) were employed whenever possible [*Banerjee et al.*, 1980; *Schmid et al.*, 1992; *Howard and Meylan*, 1997], and averages were computed if multiple estimates were available. For *cis*- and *trans*-β-ocimene, β-phellandrene, and α-terpinene we determined $K_{o/w}$ from a correlation between log$K_{o/w}$ and logδ that was developed using available estimates for other monoterpenoids emitted by *Q. ilex* ($r^2 = 0.96$). Such correlative relationships are often employed to determine either $K_{o/w}$ or δ when one of them has been experimentally determined [*Shiu and Mackay*, 1986; *Lyman*, 1990; *Schmid et al.*, 1992; *Yalkowsky and Banerjee*, 1992]. For compounds of similar structure, these correlations generally result in a good agreement between model predictions and experimental observations. Although $K_{o/w}$ of hydrophobic compounds may decrease with increasing temperature [*Lei et al.*, 2000], no data of temperature effects on $K_{o/w}$ are available for monoterpenoids.

[93] **Acknowledgments.** We thank Dr. Uwe Kuhn (Max Planck Institute for Chemistry, Mainz, Germany) for the invaluable comments. Financial support was provided by the European Commission (VOCAMOD, Contract Nr. ENV4-CT97-0424), by the Estonian Science Foundation

(Grant 4584), and by the German Federal Minister of Research and Technology (BMFT, Grants BEO 51-0339476A, EST 001-98).

References

Adams, R. P., and A. Hagerman, Diurnal variation in the volatile terpenoids of *Juniperus scopulorum* (*Cupressaceae*), *Am. J. Bot.*, *64*, 278–285, 1977.

Aubinet, M., et al., Estimates of the annual net carbon and water exchange of forests: The EUROFLUX methodology, *Adv. Ecol. Res.*, *30*, 113–175, 2000.

Ball, J. T., Calculations related to gas exchange, in *Stomatal Function*, edited by E. Zeiger, G. D. Farquhar, and I. R. Cowan, pp. 445–476, Stanford Univ. Press, Stanford, Calif., 1987.

Banerjee, S., Solubility of organic mixtures in water, *Environ. Sci. Technol.*, *18*, 587–591, 1984.

Banerjee, S., S. H. Yalkowsky, and S. C. Valvani, Water solubility and octanol/water partition coefficients of organics. Limitations of the solubility–partition coefficient correlation, *Environ. Sci. Technol.*, *14*, 1227–1229, 1980.

Bauer, K., D. Garbe, and H. Surburh, Flavors and fragrances, in *Ullmann's Encyclopedia of Industrial Chemistry. The CD-ROM Edition*, 5th ed., John Wiley, New York, 1998.

Benjamin, M. T., and A. M. Winer, Estimating the ozone-forming potential of urban trees and shrubs, *Atmos. Environ.*, *32*, 53–68, 1998.

Benjamin, M. T., M. Sudol, D. Vorsatz, and A. M. Winer, A spatially and temporally resolved biogenic hydrocarbon emissions inventory for the California South Coast Air Basin, *Atmos. Environ.*, *31*, 3087–3100, 1997.

Berezhnoi, A. N., and A. V. Semenov, *Binary Diffusion Coefficients of Liquid Vapors in Gases*, Begell House, New York, 1997.

Bertin, N., and M. Staudt, Effect of water stress on monoterpene emissions from young potted holm oak (*Quercus ilex* L.) trees, *Oecologia*, *107*, 456–462, 1996.

Bertin, N., M. Staudt, U. Hansen, G. Seufert, P. Ciccioli, P. Foster, J. L. Fugit, and L. Torres, Diurnal and seasonal course of monoterpene emissions from *Quercus ilex* (L.) under natural conditions—Applications of light and temperature algorithms, *Atmos. Environ.*, *31*, 135–144, 1997.

Büscher, K. E., Messung der Dichte, des spezifischen Volumens und des kubischen Ausdehnungskoeffizienten plastischer Massen mit Hilfe des Haake-Konsistometers, *Erdöl Kohle*, *13*, 102–106, 1960.

Calogirou, A., B. R. Larsen, C. Brussol, M. Duane, and D. Kotzias, Decomposition of terpenes by ozone during sampling on tenax, *Anal. Chem.*, *68*, 1499–1506, 1996.

Carpita, N., D. Sabularse, D. Montezinos, and D. P. Delmer, Determination of the pore size of cell walls of living plant cells, *Science*, *205*, 1144–1147, 1979.

Castro-Díez, P., P. Villar-Salvador, C. Pérez-Rontomé, M. Maestro-Martínez, and G. Montserrat-Martí, Leaf morphology and leaf chemical composition in three *Quercus* (Fagaceae) species along a rainfall gradient in NE Spain, *Trees*, *11*, 127–134, 1997.

Christodoulakis, N. S., and K. A. Mitrakos, Structural analysis of sclerophylly in eleven evergreen phanerophytes in Greece, in *Plant Response to Stress. Functional Analysis in Mediterranean Ecosystems*, *NATO ASI Ser., Ser. G: Ecol. Sci.*, vol. 15, edited by J. D. Tenhunen, F. M. Catarino, O. L. Lange, and W. C. Oechel, pp. 547–551, Springer-Verlag, New York, 1987.

Ciccioli, P., et al., Use of the isoprene algorithm for predicting the monoterpene emission from the Mediterranean holm oak *Quercus ilex* L.: Performance and limits of this approach, *J. Geophys. Res.*, *102*, 23,319–23,328, 1997.

Ciccioli, P., et al., Emission of reactive terpene compounds from orange orchards and their removal by within-canopy processes, *J. Geophys. Res.*, *104*, 8077–8094, 1999.

Daeter, W., and W. Hartung, The permeability of the epidermal cell plasma membrane of barley leaves to abscisic acid, *Planta*, *191*, 41–47, 1993.

Daubert, T. E., R. P. Danner, H. M. Sibul, and C. C. Stebbins, *Physical and Thermodynamic Properties of Pure Chemicals: Data Compilation*, Taylor and Francis, Philadelphia, Pa., 1998.

Delfine, S., O. Csiky, G. Seufert, and F. Loreto, Fumigation with exogenous monoterpenes of a non-isoprenoid-emitting oak (*Quercus suber*): Monoterpene acquisition, translocation, and effect on the photosynthetic properties at high temperatures, *New Phytol.*, *146*, 27–36, 2000.

Devon, T. K., and A. I. Scott, *Handbook of Naturally Occurring Compounds*, vol. 2, *Terpenes*, Academic, San Diego, Calif., 1972.

Diamantoglou, S., and U. Kull, Die Jahresperiodik der Fettspeicherung und ihre Beziehungen zum Kohlenhydrathaushalt bei immergrünen mediterranen Holzpflanzen, *Acta Oecol. Oecol. Plant.*, *3*, 231–248, 1982.

Dickhut, R. M., A. W. Andren, and D. E. Armstrong, Aqueous solubilities of six polychlorinated biphenyl congeners at four temperatures, *Environ. Sci. Technol.*, *20*, 807–810, 1986.

Draper, N., and H. Smith, *Applied Regression Analysis*, John Wiley, New York, 1981.

Drazer, G., R. Chertcoff, L. Bruno, and M. Rosen, Concentration dependence of diffusion–adsorption rate in activated carbon, *Chem. Eng. Sci.*, *54*, 4285–4291, 1999.

Eggersdorfer, M., Terpenes, in *Ullmann's Encyclopedia of Industrial Chemistry. The CD-ROM Edition*, 5th ed., John Wiley, New York, 1998.

Evans, J. R., S. von Caemmerer, B. A. Setchell, and G. S. Hudson, The relationship between CO_2 transfer conductance and leaf anatomy in transgenic tobacco with a reduced content of Rubisco, *Aust. J. Plant Physiol.*, *21*, 475–495, 1994.

Falk, R. H., and C. R. Stocking, Plant membranes, in *Transport in Plants*, vol. 3, *Intracellular Interactions and Transport Processes*, edited by C. R. Stocking and U. Heber, pp. 3–50, Springer-Verlag, New York, 1976.

Farquhar, G. D., and T. D. Sharkey, Stomatal conductance and photosynthesis, *Annu. Rev. Plant Physiol.*, *33*, 317–345, 1982.

Fehsenfeld, F., et al., Emissions of volatile organic compounds from vegetation and the implications for atmospheric chemistry, *Global Biogeochem. Cycles*, *6*, 389–430, 1992.

Fichan, I., C. Larroche, and J. B. Gros, Water solubility, vapor pressure, and activity coefficients of terpenes and terpenoids, *J. Chem. Eng. Data*, *44*, 56–62, 1999.

Field, C. B., J. T. Ball, and J. A. Berry, Photosynthesis: Principles and field techniques, in *Plant Physiological Ecology. Field Methods and Instrumentation*, edited by R. W. Pearcy, J. R. Ehleringer, H. A. Mooney, and P. W. Rundel, pp. 209–253, Chapman and Hall, London, 1989.

Fluka Chemie AG, *Laboratory Chemicals and Analytical Reagents*, Fluka Chemie AG-RdH Laborchemikalien GmbH & Co. KG, Deisenhofen, 1999.

Fuentes, J. D., D. Wang, H. H. Neumann, T. J. Gillespie, G. den Hartog, and T. F. Dann, Ambient biogenic hydrocarbons and isoprene emissions from a mixed deciduous forest, *J. Atmos. Chem.*, *25*, 67–95, 1996.

Fuentes, J. D., et al., Biogenic hydrocarbons in the atmospheric boundary layer: A review, *Bull. Am. Meteorol. Soc.*, *81*, 1537–1575, 2000.

Fugmann, B., S. Lang-Fugmann, and W. Steglich (Eds.), *Römpp Lexikon: Naturstoffe*, Georg Thieme Verlag, Stuttgart, 1997.

Geron, C., R. Rasmussen, R. R. Arnts, and A. Guenther, A review and synthesis of monoterpene speciation from forests in the United States, *Atmos. Environ.*, *34*, 1761–1781, 2000.

Gimmler, H., B. Heilmann, B. Demmig, and W. Hartung, The permeability coefficients of the plasmalemma and the chloroplast envelope of spinach mesophyll cells for phytohormones, *Z. Naturforsch. C*, *36*, 672–678, 1981.

Grain, C. F., Activity coefficient, in *Handbook of Chemical Property Estimation Methods. Environmental Behavior of Organic Compounds*, edited by W. J. Lyman, W. F. Reehl, and D. H. Rosenblatt, pp. 11/1–11/53, Am. Chem. Soc., Washington, D. C., 1990a.

Grain, C. F., Vapor pressure, in *Handbook of Chemical Property Estimation Methods. Environmental Behavior of Organic Compounds*, edited by W. J. Lyman, W. F. Reehl, and D. H. Rosenblatt, pp. 14/1–14/20, Am. Chem. Soc., Washington, D. C., 1990b.

Gratani, L., Structural and ecophysiological plasticity of some evergreen species of the Mediterranean maquis in response to climate, *Photosynthetica*, *31*, 335–343, 1995.

Gratani, L., and E. Fiorentino, Variations in leaf characteristics of *Quercus ilex* L. over a microclimatic gradient, *Photosynthetica*, *22*, 228–231, 1988.

Gratani, L., E. Fiorentino, A. Kubová, and P. Marzi, Effect of microclimate on ecophysiological features of some sclerophyllous species, *Photosynthetica*, *23*, 230–233, 1989.

Grossoni, P., F. Bussotti, C. Tani, E. Gravano, S. Santarelli, and A. Bottacci, Morpho-anatomical alterations in leaves of *Fagus sylvatica* L. and *Quercus ilex* L. in different environmental stress conditions, *Chemosphere*, *36*, 919–924, 1998.

Guenther, A., P. R. Zimmerman, and M. Wildermuth, Natural volatile organic compound emission rates for U. S. woodland landscapes, *Atmos. Environ.*, *28*, 1197–1210, 1994.

Guenther, A., et al., A global model of natural volatile compound emissions, *J. Geophys. Res.*, *100*, 8873–8892, 1995.

Guenther, A., J. Greenberg, P. Harley, D. Helmig, L. Klinger, L. Vierling, P. Zimmerman, and C. Geron, Leaf, branch, stand and landscape scale measurements of volatile organic compound fluxes from U.S. woodlands, *Tree Physiol.*, *16*, 17–24, 1996.

Guenther, A., C. Geron, T. Pierce, B. Lamb, P. Harley, and R. Fall, Natural emissions of non-methane volatile organic compounds, carbon monoxide, and oxides of nitrogen from North America, *Atmos. Environ.*, *34*, 2205–2230, 2000.

Guenther, A. B., R. K. Monson, and R. Fall, Isoprene and monoterpene emission rate variability: Observations with *Eucalyptus* and emission rate algorithm development, *J. Geophys. Res.*, *96*, 10,799–10,808, 1991.

Guenther, A. B., P. R. Zimmerman, P. C. Harley, R. K. Monson, and R. Fall, Isoprene and monoterpene emission rate variability: Model evaluations and sensitivity analyses, *J. Geophys. Res.*, *98*, 12,609–12,617, 1993.

Hakola, H., J. Rinne, and T. Laurila, The hydrocarbon emission rates of tea-leafed willow (*Salix phylicifolia*), silver birch (*Betula pendula*) and European aspen (*Populus tremula*), *Atmos. Environ.*, *32*, 1825–1833, 1998.

Hansen, U., and G. Seufert, Terpenoid emission from *Citrus sinensis* (L.) OSBECK under drought stress, *Phys. Chem. Earth, Part B*, *42*, 681–687, 1999.

Hayduk, W., and H. Laudie, Prediction of diffusion coefficients for non-electrolytes in dilute aqueous solutions, *J. Am. Inst. Chem. Eng.*, *20*, 611–615, 1974.

Heber, U., and H. W. Heldt, The chloroplast envelope: Structure, function, and role in leaf metabolism, *Annu. Rev. Plant Physiol.*, *32*, 139–168, 1981.

Heiden, A. C., K. Kobel, and J. Wildt, *Einfluß verschiedener Stre*β*faktoren auf die Emission pflanzlicher flüchtiger organischer Verbindungen*, *Ber. Forschungzentrum Jülich*, vol. 3622, Institut für Chemie und Dynamik der Geosphäre 2: Chemie der Belasteten Atmosphäre, Forschungszentrum Jülich, Jülich, 1999.

Howard, P. H., and W. M. Meylan (Eds.), *Handbook of Physical Properties of Organic Chemicals*, Lewis Publishers, Boca Raton, Fla., 1997.

Jordan, T. E., *Vapor Pressure of Organic Compounds*, Wiley-Interscience, New York, 1954.

Jørgensen, R. B., O. Bjørseth, and B. Malavik, Chamber testing of adsorption of volatile organic compounds (VOC) on material surfaces, *Indoor Air*, *9*, 2–9, 1999.

Josephy, E., and F. Radt (Eds.), *Carboisocyclic Condensed Compounds, 3, Elsevier's Encyclopaedia of Organic Chemistry*, vol. 12A, *Bicyclic Compounds (Except Naphthalene)*, Elsevier Sci., New York, 1948.

Kesselmeier, J., et al., Emission of short chained organic acids, aldehydes and monoterpenes from *Quercus ilex* L. and *Pinus pinea* L. in relation to physiological activities, carbon budget and emission algorithms, *Atmos. Environ.*, *31*, 119–133, 1997.

Kesselmeier, J., et al., Simultaneous field measurements of terpene and isoprene emissions from two dominant Mediterranean oak species in relation to a north American species, *Atmos. Environ.*, *32*, 1947–1953, 1998.

Laisk, A., and V. Oja, *Techniques in Plant Sciences, 1, Dynamics of Leaf Photosynthesis: Rapid-Response Measurements and Their Interpretations*, CSIRO Publishing, Canberra, 1998.

Laisk, A., O. Kiirats, and V. Oja, Assimilatory power (postillumination CO_2 uptake) in leaves, *Plant Physiol.*, *76*, 723–729, 1984.

Lee, X., On micrometeorological observations of surface-air exchange over tall vegetation, *Agric. For. Meteorol.*, *91*, 39–49, 1998.

Lei, Y. D., F. Wania, W. Y. Shiu, and D. G. B. Boocock, HPLC-based method for estimating the temperature dependence of *n*-octanol–water partition coefficients, *J. Chem. Eng. Data*, *45*, 738–742, 2000.

Lerdau, M., S. B. Dilts, H. Westberg, B. K. Lamb, and E. J. Allwine, Monoterpene emission from ponderosa pine, *J. Geophys. Res.*, *99*, 16,609–16,615, 1994.

Leuning, R., Transport of gases into leaves, *Plant Cell Environ.*, *6*, 181–194, 1983.

Lide, D. R., and H. Kehiaian, *CRC Handbook of Thermophysical and Thermochemical Data*, CRC Press, Boca Raton, Fla., 1994.

Logan, B. A., R. K. Monson, and M. J. Potosnak, Biochemistry and physiology of foliar isoprene production, *Trends Plant Sci.*, *5*, 477–481, 2000.

Loreto, F., and T. D. Sharkey, On the relationship between isoprene emission and photosynthetic metabolites under different environmental conditions, *Planta*, *189*, 420–424, 1993.

Loreto, F., P. Ciccioli, E. Brancaleoni, A. Cecinato, M. Frattoni, and T. D. Sharkey, Different sources of reduced carbon contribute to form three classes of terpenoid emitted by *Quercus ilex* L. leaves, *Proc. Natl. Acad. Sci. U. S. A.*, *93*, 9966–9969, 1996a.

Loreto, F., P. Ciccioli, A. Cecinato, E. Brancaleoni, M. Frattoni, C. Fabozzi, and D. Tricoli, Evidence of the photosynthetic origin of monoterpenes emitted by *Quercus ilex* L. leaves by ^{13}C labeling, *Plant Physiol.*, *110*, 1317–1322, 1996b.

Loreto, F., P. Ciccioli, A. Cecinato, E. Brancaleoni, M. Frattoni, and D. Tricoli, Influence of environmental factors and air composition on the emission of α-pinene from *Quercus ilex* leaves, *Plant Physiol.*, *110*, 267–275, 1996c.

Loreto, F., P. Ciccioli, E. Brancaleoni, A. Cecinato, and M. Frattoni, Measurement of isoprenoid content in leaves of Mediterranean *Quercus* spp. by a novel and sensitive method and estimation of the isoprenoid partition between liquid and gas phase inside the leaves, *Plant Sci.*, *136*, 25–30, 1998.

Loreto, F., P. Ciccioli, E. Brancaleoni, M. Frattoni, and S. Delfine, Incomplete ^{13}C labelling of α-pinene content of *Quercus ilex* leaves and appearance of unlabelled C in α-pinene emission in the dark, *Plant Cell Environ.*, *23*, 229–234, 2000.

Lyman, W. J., Solubility in water, in *Handbook of Chemical Property Estimation Methods. Environmental Behavior of Organic Compounds*, edited by W. J. Lyman, W. F. Reehl, and D. H. Rosenblatt, pp. 2/1–2/52, Am. Chem. Soc., Washington, D. C., 1990.

Mackay, D., and W. Y. Shiu, A critical review of Henry's law constants for chemicals of environmental interest, *J. Phys. Chem. Ref. Data*, *19*, 1175–1199, 1981.

Manes, F., A. Grignetti, A. Tinelli, R. Lenz, and P. Ciccioli, General features of the Castelporziano test site, *Atmos. Environ.*, *31*, 19–25, 1997.

Martin, M. J., C. M. Stirling, S. W. Humphries, and S. P. Long, A process-based model to predict the effects of climatic change on leaf isoprene emission rates, *Ecol. Modell.*, *131*, 161–174, 2000.

Massaldi, H. A., and C. J. King, Simple technique to determine solubilities of sparingly soluble organics: Solubility and activity coefficients of *d*-limonene, *n*-butylbenzene, and *n*-hexyl acetate in water and sucrose solutions, *J. Chem. Eng. Data*, *18*, 393–397, 1973.

Maurel, C., Aquaporins and water permeability of plant membranes, *Annu. Rev. Plant Physiol. Plant Mol. Biol.*, *48*, 399–429, 1997.

McAuliffe, C., Solubility in water of normal C_9 and C_{10} alkane hydrocarbons, *Science*, *163*, 478–479, 1969.

Merck KGaA, *Chemical Reagents 1999/2000*, Merck KGaA, Darmstadt, 1999.

Moncrieff, J., R. Valentini, S. Greco, G. Seufert, and P. Ciccioli, Trace gas exchange over terrestrial ecosystems: Methods and perspectives in micrometeorology, *J. Exp. Bot.*, *48*, 1133–1142, 1997.

Monson, R. K., and R. Fall, Isoprene emission from aspen leaves. Influence of environment and relation to photosynthesis and photorespiration, *Plant Physiol.*, *90*, 267–274, 1989.

Monson, R. K., M. T. Lerdau, T. D. Sharkey, D. S. Schimel, and R. Fall, Biological aspects of constructing volatile organic compound emission inventories, *Atmos. Environ.*, *29*, 2989–3002, 1995.

Müller, J.-F., Geoographical distribution and seasonal variation of surface emissions and deposition velocities of atmospheric trace gases, *J. Geophys. Res.*, *97*, 3787–3804, 1992.

Myrdal, P. B., A. M. Manka, and S. H. Yalkowsky, AQUAFAC 3: Aqueous functional group activity coefficients: Application to the estimation of aqueous solubility, *Chemosphere*, *30*, 1619–1637, 1995.

Nelken, L. H., Densities of vapors, liquids and solids, in *Handbook of Chemical Property Estimation Methods. Environmental Behavior of Organic Compounds*, edited by W. J. Lyman, W. F. Reehl, and D. H. Rosenblatt, pp. 19/1–19/24, Am. Chem. Soc., Washington, D. C., 1990.

Niinemets, Ü., J. D. Tenhunen, P. C. Harley, and R. Steinbrecher, A model of isoprene emission based on energetic requirements for isoprene synthesis and leaf photosynthetic properties for *Liquidambar* and *Quercus*, *Plant Cell Environ.*, *22*, 1319–1336, 1999.

Niinemets, Ü., K. Hauff, N. Bertin, J. D. Tenhunen, R. Steinbrecher, and G. Seufert, Monoterpene emissions in relation to foliar photosynthetic and structural variables in Mediterranean evergreen *Quercus* species, *New Phytol.*, *153*, 243–256, 2002a.

Niinemets, Ü., M. Reichstein, M. Staudt, G. Seufert, and J. D. Tenhunen, Stomatal constraints may affect emission of oxygenated monoterpenoids from the foliage of *Pinus pinea*, *Plant Physiol.*, *130*, 1371–1385, 2002b.

Niinemets, Ü., G. Seufert, R. Steinbrecher, and J. D. Tenhunen, A model coupling foliar monoterpene emissions to leaf photosynthetic characteristics in Mediterranean evergreen *Quercus* species, *New Phytol.*, *153*, 257–276, 2002c.

Nobel, P. S., *Physicochemical and Environmental Plant Physiology*, 4th ed., Academic, San Diego, Calif., 1991.

Owen, S., C. Boissard, R. A. Street, S. C. Duckham, O. Csiky, and C. N. Hewitt, Screening of 18 Mediterranean plant species for volatile organic compound emissions, *Atmos. Environ.*, *31*, 101–117, 1997.

Paoletti, E., UV-B and acid rain effects on beech (*Fagus sylvatica* L.) and holm oak (*Quercus ilex* L.) leaves, *Chemosphere*, *36*, 835–840, 1998.

Parkhurst, D. F., Tansley review no. 65. Diffusion of CO_2 and other gases inside leaves, *New Phytol.*, *126*, 449–479, 1994.

Peñuelas, J., and J. Llusià, Seasonal emission of monoterpenes by the Mediterranean tree *Quercus ilex* in field conditions: Relations with photosynthetic rates, temperature and volatility, *Physiol. Plant.*, *105*, 641–647, 1999a.

Peñuelas, J., and J. Llusià, Short-term responses of terpene emission rates to experimental changes of PFD in *Pinus halepensis* and *Quercus ilex* in summer field conditions, *Environ. Exp. Bot.*, *42*, 61–68, 1999b.

Pio, C., C. Alves, and A. Duarte, Organic components of aerosols in a forested area of central Greece, *Atmos. Environ.*, *35*, 389–401, 2001.

Prasetyo, I., H. D. Do, and D. D. Do, Surface diffusion of strong adsorbing vapours on porous carbon, *Chem. Eng. Sci.*, *57*, 133–141, 2002.

Rice, C. P., S. M. Chernyak, and L. L. McConnell, Henry's law constants for pesticides measured as a function of temperature and salinity, *J. Agric. Food Chem.*, *45*, 2291–2298, 1997.

Sabillón, D., and L. V. Cremades, Diurnal and seasonal variation of monoterpene emission rates for typical Mediterranean species (*Pinus pinea* and *Quercus ilex*) from field measurements—Relationship with temperature and PAR, *Atmos. Environ.*, *35*, 4419–4431, 2001.

Sangster, J., Octanol–water partition coefficients of simple organic compounds, *J. Phys. Chem. Ref. Data*, *18*, 111–229, 1989.

Schmid, C., Sorptions- und Permeationseigenschaften der pflanzlichen Kutikula für Monoterpene, Dr. rer. Nat. thesis, Tech. Univ. München, 1991.

Schmid, C., R. Steinbrecher, and H. Ziegler, Partition coefficients of plant cuticles for monoterpenes, *Trees*, *6*, 32–36, 1992.

Schönherr, J., and P. Baur, Modelling penetration of plant cuticles by crop protection agents and the effects of adjuvants on their rates of penetration, *Pestic. Sci.*, *42*, 185–208, 1994.

Schreiber, L., T. Kirsch, and M. Riederer, Transport properties of cuticular waxes of *Fagus sylvatica* L. and *Picea abies* (L.) Karst.: Estimation of size selectivity and tortuosity from diffusion coefficients of aliphatic molecules, *Planta*, *198*, 104–109, 1996.

Schuh, G., A. C. Heiden, T. Hoffmann, J. Kahl, P. Rockel, J. Rudolph, and J. Wildt, Emissions of volatile organic compounds from sunflower and beech: Dependence on temperature and light intensity, *J. Atmos. Chem.*, *27*, 291–318, 1997.

Schürmann, W., H. Ziegler, D. Kotzias, R. Schönwitz, and R. Steinbrecher, Emission of biosynthesized monoterpenes from needles of Norway spruce, *Naturwissenschaften*, *80*, 276–278, 1993.

Shao, M., K. V. Czapiewski, A. C. Heiden, K. Kobel, M. Komenda, R. Koppmann, and J. Wildt, Volatile organic compound emissions from Scots pine: Mechanisms and description by algorithms, *J. Geophys. Res.*, *106*, 20,483–20,491, 2001.

Sharkey, T. D., and F. Loreto, Water stress, temperature, and light effects on the capacity for isoprene emission and photosynthesis of kudzu leaves, *Oecologia*, *95*, 328–333, 1993.

Shiu, W. Y., and D. Mackay, A critical review of aqueous solubilities, vapor pressures, Henry's law constants, and octanol–water partition coefficients of the polychlorinated biphenyls, *J. Phys. Chem. Ref. Data*, *15*, 911–929, 1986.

Simon, V., B. Clement, M. L. Riba, and L. Torres, The Landes experiment: monoterpenes emitted from maritime pine, *J. Geophys. Res.*, *99*, 16,501–16,510, 1994.

Singsaas, E. L., and T. D. Sharkey, The effects of high temperature on isoprene synthesis in oak leaves, *Plant Cell Environ.*, *23*, 751–757, 2000.

Singsaas, E. L., M. M. Laporte, J.-Z. Shi, R. K. Monson, D. R. Bowling, K. Johnson, M. Lerdau, A. Jasentuliytana, and T. D. Sharkey, Kinetics of leaf temperature fluctuation affect isoprene emission from red oak (*Quercus rubra*) leaves, *Tree Physiol.*, *19*, 917–924, 1999.

Sotelo, J. L., G. Ovejero, J. A. Delgado, and I. Martinez, Comparison of adsorption equilibrium and kinetics of four chlorinated organics from water onto GAC, *Water Res.*, *36*, 599–608, 2002.

Staudinger, J., and P. V. Roberts, A critical review of Henry's law constants for environmental applications, *Crit. Rev. Environ. Sci. Technol.*, *26*, 205–297, 1996.

Staudt, M., and N. Bertin, Light and temperature dependence of the emission of cyclic and acyclic monoterpenes from holm oak (*Quercus ilex* L.) leaves, *Plant Cell Environ.*, *21*, 385–395, 1998.

Staudt, M., N. Bertin, U. Hansen, G. Seufert, P. Ciccioli, P. Foster, B. Frenzel, and J.-L. Fugit, Seasonal and diurnal patterns of monoterpene emissions from *Pinus pinea* (L.) under field conditions, *Atmos. Environ.*, *31*, 145–156, 1997.

Staudt, M., N. Bertin, B. Frenzel, and G. Seufert, Seasonal variation in amount and composition of monoterpenes emitted by young *Pinus pinea* trees—Implications for emission modeling, *J. Atmos. Chem.*, *35*, 77–99, 2000.

Staudt, M., N. Mandl, R. Joffre, and S. Rambal, Intraspecific variability of monoterpene composition emitted by *Quercus ilex* leaves, *Can. J. For. Res.*, *31*, 174–180, 2001.

Syvertsen, J. P., J. Lloyd, C. McConchie, P. E. Kriedemann, and G. D. Farquhar, On the relationship between leaf anatomy and CO_2 diffusion through the mesophyll of hypostomatous leaves, *Plant Cell Environ.*, *18*, 149–157, 1995.

Terashima, I., M. Ishibashi, K. Ono, and K. Hikosaka, Three resistances to CO_2 diffusion: leaf-surface water, intercellular spaces and mesophyll cells, in *Photosynthesis: From Light to Biosphere*, vol. 5, edited by P. Mathis, pp. 537–542, Kluwer Acad., Norwell, Mass., 1995.

Terradas, J., and R. Savé, The influence of summer and winter stress and water relationships on the distribution of *Quercus ilex* L., *Vegetatio*, *99–100*, 137–145, 1992.

Thomas, R. G., Volatilization from water, in *Handbook of Chemical Property Estimation Methods. Environmental Behavior of Organic Compounds*, edited by W. J. Lyman, W. F. Reehl, and D. H. Rosenblatt, pp. 15/1–15/34, Am. Chem. Soc., Washington, D. C., 1990.

Tingey, D. T., D. P. Turner, and J. A. Weber, Factors controlling the emissions of monoterpenes and other volatile organic compounds, in *Physiological Ecology. A Series of Monographs, Texts, and Treatises: Trace Gas Emissions by Plants*, edited by T. D. Sharkey, E. A. Holland, and H. A. Mooney, pp. 93–119, Academic, San Diego, Calif., 1991.

Tinoco-Ojanguren, C., and R. W. Pearcy, Stomatal dynamics and its importance to carbon gain in two rainforest *Piper* species, 2, Stomatal versus biochemical limitations during photosynthetic induction, *Oecologia*, *94*, 395–402, 1993.

Tretiach, M., G. Bolognini, and A. Rondi, Photosynthetic activity of *Quercus ilex* at the extremes of a transect between Mediterranean and submediterranean vegetation (Trieste—NE Italy), *Flora*, *192*, 369–378, 1997.

Tucker, W. A., and L. H. Nelken, Diffusion coefficients in air and water, in *Handbook of Chemical Property Estimation Methods. Environmental Behavior of Organic Compounds*, edited by W. J. Lyman, W. F. Reehl, and D. H. Rosenblatt, pp. 17/1–17/25, McGraw-Hill, New York, 1982.

Valentini, R., G. Scarascia-Mugnozza, and J. R. Ehleringer, Hydrogen and carbon isotope ratios of selected species of a Mediterranean macchia ecosystem, *Funct. Ecol.*, *6*, 627–631, 1992.

Valentini, R., S. Greco, G. Seufert, N. Bertin, P. Ciccioli, A. Cecinato, E. Brancaleoni, and M. Frattoni, Fluxes of biogenic VOC from Mediterranean vegetation by trap enrichment relaxed eddy accumulation, *Atmos. Environ.*, *31*, 229–238, 1997.

Vargaftik, N. B., *Spravochnik po teplofizicheskim svoistvam gazov i zhidkostei*, 2nd ed., Nauka, Moscow, 1972.

Visual Numerics, *PV-Wave Advantage Reference*, Visual Numerics, Houston, Tex., 1993.

von Caemmerer, S., and D. L. Edmondson, Relationship between steady-state gas exchange, *in vivo* ribulose bisphosphate carboxylase activity and some carbon reduction cycle intermediates in *Raphanus sativum*, *Aust. J. Plant Physiol.*, *13*, 669–688, 1986.

Wagner, J., S. Pelaez Menendez, and W. Larcher, Bioclimate and productive potential of *Quercus ilex* L. at its northernmost distribution limit, 3, Morphological and functional adaptations of leaves to their light regime (in Italian), *Studi Trentini Sci. Nat., Acta Biol*, *68*, 37–51, 1993.

Weast, R. C., D. R. Lide, M. J. Astle, and W. H. Beyer (Eds.), *CRC Handbook of Chemistry and Physics. A Ready-Reference Book of Chemical and Physical Data*, 70th ed., CRC Press, Boca Raton, Fla., 1989.

Weidenhamer, J. D., F. A. Macias, N. H. Fischer, and G. B. Williamson, Just how insoluble are monoterpenes?, *J. Chem. Ecol.*, *19*, 1799–1807, 1993.

Weier, T. E., C. R. Stocking, and L. K. Shumway, The photosynthetic apparatus in chloroplasts of higher plants, in *Energy Conversion by the Photosynthetic Apparatus. Report of Symposium Held June 6–9, 1966*, *Brookhaven Symp. Biol*, vol. 19, edited by J. M. Olson, G. Hind, H. Lyman, and H. W. Siegelman, pp. 353–374, Biol. Dep., Brookhaven Natl. Lab., Upton, N. Y., 1967.

Weisiger, R. A., Impact of extracellular and intracellular diffusion barriers on transport, in *Whole Organ Approach to Cellular Metabolism*, edited by J. B. Bassingthwaighte, C. A. Goresky, and J. H. Linehan, pp. 389–423, Springer-Verlag, New York, 1998.

Weitz, H. M., and E. Loser, Isoprene, in *Ullmann's Encyclopedia of Industrial Chemistry. The CD-ROM Edition*, 5th ed., John Wiley, New York, 1998.

Wilke, C. R., and C. Y. Lee, Estimation of diffusion coefficients for gases and vapors, *Ind. Eng. Chem.*, *47*, 1253–1257, 1955.

Yalkowsky, S. H., and S. Banerjee, *Aqueous Solubility. Methods of Estimation for Organic Compounds*, Marcel Dekker, New York, 1992.

Yeletskii, A. V., Vyazkost, in *Fizicheskiye velichiny. Spravochnik*, edited by I. S. Grigoryeva and E. Z. Meilihova, pp. 364–374, Energoatomizdat, Moscow, 1991.

Ü. Niinemets, Department of Plant Physiology, Institute of Molecular and Cell Biology, Riia 23, EE 51010 Tartu, Estonia. (ylo@zbi.ee)

M. Reichstein, Department of Plant Ecology, University of Bayreuth, D-95440 Bayreuth, Germany.